

Design of a Next Generation Military Heavy-Lift Air Transport

a project presented to
The Faculty of the Department of Aerospace Engineering
San José State University

in partial fulfillment of the requirements for the degree
Master of Science in Aerospace Engineering

by

Brian H. Andrade

December 2017

approved by

Dr. Nikos J. Mourtos
Faculty Advisor



San José State
UNIVERSITY

Design of a Next Generation Military Heavy-Lift Air Transport

Brian H Andrade¹

This paper outlines the preliminary class I design, class I design reevaluation, and the beginning of the class II design of a new military heavy lift air transport, the “Goliath,” to replace the aging C-5 at the end of its service life. This aircraft has been designed to meet both FAR 25 and Military aircraft design standards. The design represents an apparently viable design at this stage of the design and analysis process. The design meets ICAO category V restrictions while providing improved payload, range and cost over the currently operational C-5M “Galaxy”.

Table of Contents

Design of a Next Generation Military Heavy-Lift Air Transport	1
I. Introduction.....	4
II. Project Schedule	4
III. Motivation and Literature Review	6
IV. Mission Specifications.....	9
V. Class I Design Overview	9
A. Configuration.....	9
B. Weight Sizing and Sensitivities	10
C. Performance Analysis.....	11
D. Fuselage Design.....	11
E. Wing Design.....	11
F. Empennage Design.....	12
G. Landing Gear	13
H. Stability and Control.....	13
VI. Class I Reevaluation	14
VII. Class II Landing Gear and Tire Design	17
VIII. Preliminary Structural Arrangement	18
IX. V-N Diagram.....	20
X. Class II Weight Estimation	21
XI. Reassessed Drag Polars	25
XII. Propulsion Characteristics	25
XIII. Performance Evaluation	27
A. Takeoff.....	28
.....	28

¹ Master’s Student, San Jose State University Aerospace Engineering, One Washington Square San Jose CA, Student

B. Cruise.....	29
C. Landing.....	31
XIV. Cost and Maintenance Evaluation.....	33
XV. Final Geometry.....	34
A. Wing.....	34
B. Horizontal Stabilizer.....	36
XVI. Discussion.....	41
XVII. Conclusion.....	41
References.....	43

Table of Figures

Figure 1. Projected Project Schedule.....	5
Figure 2. Proposed Hydrogen Powered Cargo Aircraft.....	6
Figure 3. Recent Proposed LH ₂ Powerd Aircraft.....	7
Figure 4. Nuclear Powered Aircraft Concept.....	8
Figure 5. Mission Profile.....	9
Figure 6. Wing Sweep and Thickness Trade Study.....	12
Figure 7. Side View of the Vertical Stabilizer. Geometric breakdown of the vertical stabilizer.....	12
Figure 8. Planform View of the Horizontal Tail. Geometric layout of the horizontal tail.....	13
Figure 9. Longitudinal X-plot.....	13
Figure 10. Historic Skin Friction Coefficients.....	15
Figure 11. Class I Drag Polars.....	15
Figure 12. Revised Aircraft Geometry.....	16
Figure 13. ESWL and LCN Graph.....	17
Figure 14. Partial Outline of Preliminary Structural Elements.....	19
Figure 15. V-n Diagram. Basic V-n diagram for the Goliath.....	20
Figure 16. Engine Weight Estimation Trend.....	22
Figure 17. Reassessed Drag Polar.....	25
Figure 18. Approximate Thrust-Speed Characteristics at SL.....	27
Figure 19. Takeoff Field Geometry.....	29
Figure 20. Thrust Available vs Required.....	30
Figure 21. Payload vs. Range.....	31
Figure 22. Basic Wing Planform.....	34
Figure 23. Wing Devices Layout.....	35
Figure 24. Basic Horizontal Stabilizer Planform Area.....	36
Figure 25. Horizontal Stabilizer Control Surface Layout.....	37
Figure 26. Vertical Stabilizer Basic Layout.....	38
Figure 27. Vertical Stabilizer Control Surface Layout.....	39
Figure 28. AAA Three-view.....	40
Table 1. HUULC Aircraft Data.....	7
Table 2. Heinze and Hepperle Data Summary.....	8
Table 3. Aircraft Specifications.....	9
Table 4. Aircraft Configuration Comparisions.....	10
Table 5. Mission Fuel Use Breakdown.....	10
Table 6. Weight Sensitivity Summary.....	11
Table 7. Weight Sensitivity Summary.....	14
Table 8. Class II Structual Component Weights.....	21
Table 9. Class II Fixed Equip. Component Weights.....	23
Table 10. Class II Center of Gravity Table.....	24
Table 11. Aircraft Specifications.....	27
Table 12. Analysis of Key Performance Parameters.....	32
Table 13. Cost Breakdown.....	33

I. Introduction

THIS paper is an overview of the work and results of the preliminary design for a next generation military heavy-lift air transport. The work during spring 2016 encompassed the class I design of the aircraft up through the preliminary drag polars and proves that the design point chosen is a viable one for the level of technology chosen for this aircraft.

The work during spring 2017 reevaluates some of the aspects of the preliminary design to address important remaining issues, verifies the class I design, and moves into the class II design of the aircraft. The work to date in class II design covers class II design of landing gear and tires, a preliminary structural arrangement, a V-n diagram and the beginning of class II weight and balance estimations.

II. Project Schedule

This project is a year-long project to execute the class II design of a next generation military air transport in partial satisfaction of the requirements for a Masters of Science in Aerospace Engineering. This project began as a semester project for a course on advanced aircraft design and was extended in scope to satisfy the requirements of a master's project. The schedule for this project beginning Spring 2017 starts at the beginning of the class II design as outlined by Roskam¹ and moves through the end of this design sequence by the end of Fall 2017. A schedule estimate of this project can be found in the gantt chart of figure 1 on the next page.

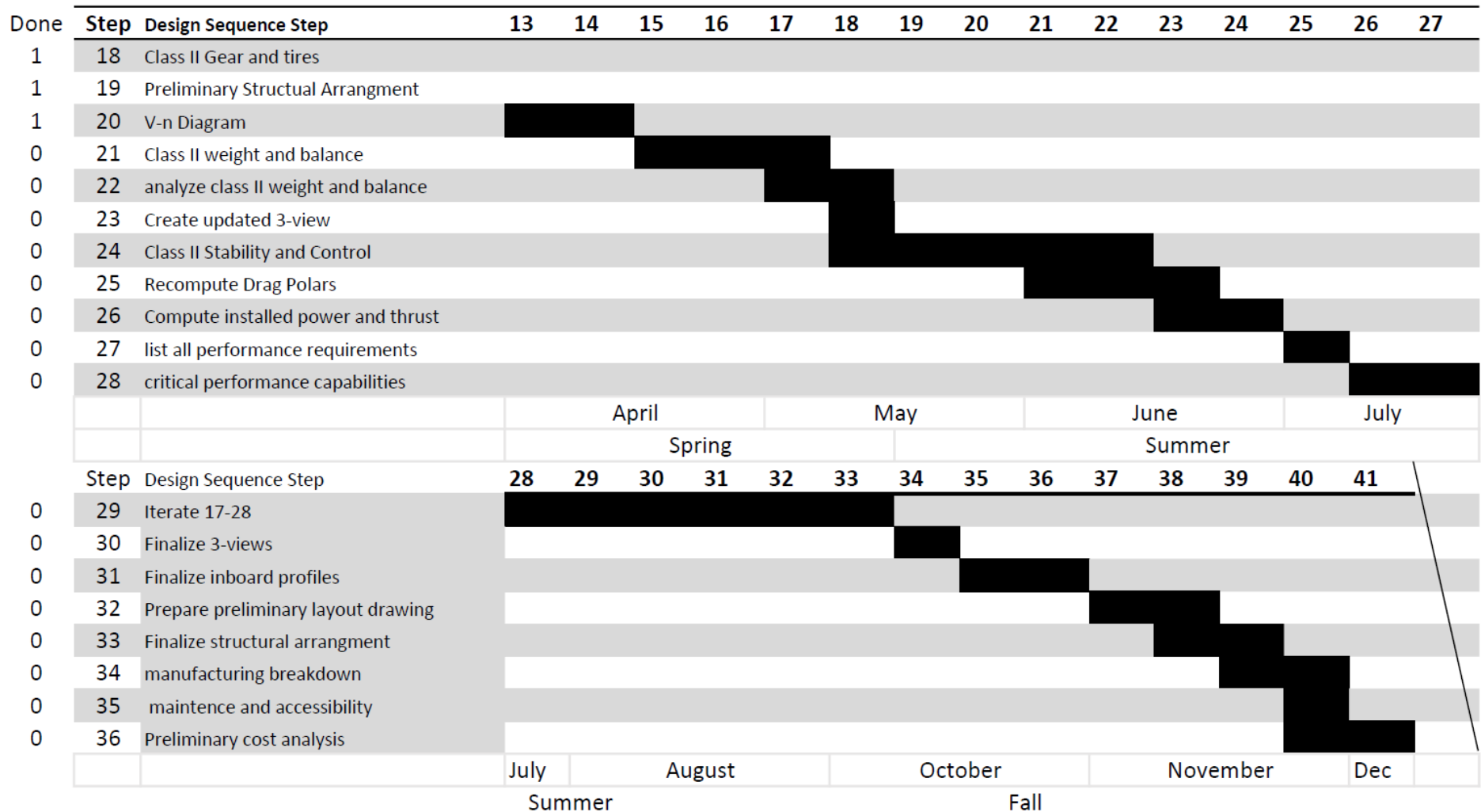


Figure 1. Projected Project Schedule. A predicted schedule of the project outlining the duration and sequence of steps in class II aircraft design as outlined by Roskam¹.

III. Motivation and Literature Review

The C-5 “Galaxy” first entered production in 1968, with the latest airframes produced in 1989. More recently the C-5 fleet has undergone a refit program to extend the service life to 2040.² However, with the historically long design and manufacturing phases for United States military aircraft, it is necessary to begin the design phase in order to have a viable replacement aircraft at the C-5’s end of service. For comparison, the F-35 began its process in 1997 when Lockheed Martin was selected for the Joint Strike Fighter concept demonstration phase; the F-35 entered active service in July of 2015.³

The timeline is not the only motivating factor for a next generation military heavy lift transport. When it was introduced, the C-5 was capable of carrying two M1 Abrams main battle tanks (MBT). With the most recent version of the M1 platform, the M1A2 SEP, weighing almost 24000 lb more than the original M1, the C-5 is no longer capable of carrying a pair of modern MBTs; this results in approximately a 25% decrease in the military airlift capacity for MBT’s (factoring in all MBT capable aircraft).⁴

Additionally, with the change in the worldwide military situation, a set piece battle of conventional forces between NATO and former Warsaw Pact nation forces is all but unthinkable. Instead, military operations are conducted in more remote territories where infrastructure is far less considerable than that found in the staging areas of the European theatre. As such, a successor to the C-5 which improved its landing and takeoff field length and range would be invaluable in reorienting the military airlift capacity of the United States towards modern challenges while retaining traditional capabilities.

Finally, when the C-5 was designed and introduced, the power, efficiency and physical envelope of turbofan jet engines were all much lower and smaller than they are today. These limitations required the use of four of the biggest engines then available for the initial design. With advances in engine design an aircraft of similar scale would have vastly improved performance and efficiency. Some effort has been made to employ these benefits in the form of the C-5M refit program, however, fundamental design choices remain in the form of wing structure and load distribution. To fully utilize both modern engines, materials and avionics as well as leverage modern analytical and design processes, a new military heavy lift transport must be developed from the ground up.

A significant amount of work has gone into the investigation of new large military cargo transports. However, much of this work is old and no data on recent developments was found outside of purely theoretical contexts. This is expected since the development of a new military heavy transport would likely be classified due to the militarily strategic nature of such an aircraft.

Many of the concepts found in literature center around unconventional designs, either in their propulsion system or the configuration. Some of the earliest examples found for literature investigating this area looked at both nuclear and liquid hydrogen powered aircraft of conventional and flying wing configurations.⁵ However, due to the requirements for integration with existing infrastructure and safety concerns, both designs were deemed infeasible.

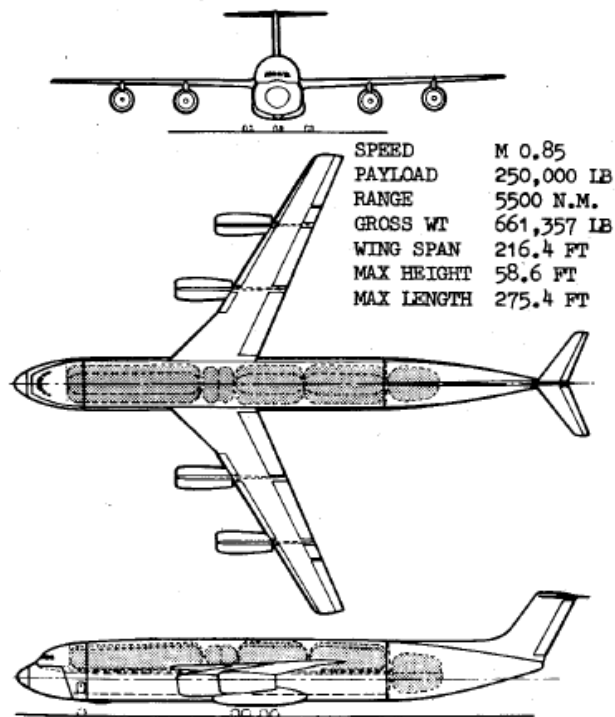


Figure 2. Proposed Hydrogen Powered Cargo Aircraft. *Hydrogen powered cargo aircraft concept presented in the 1970's.*⁵

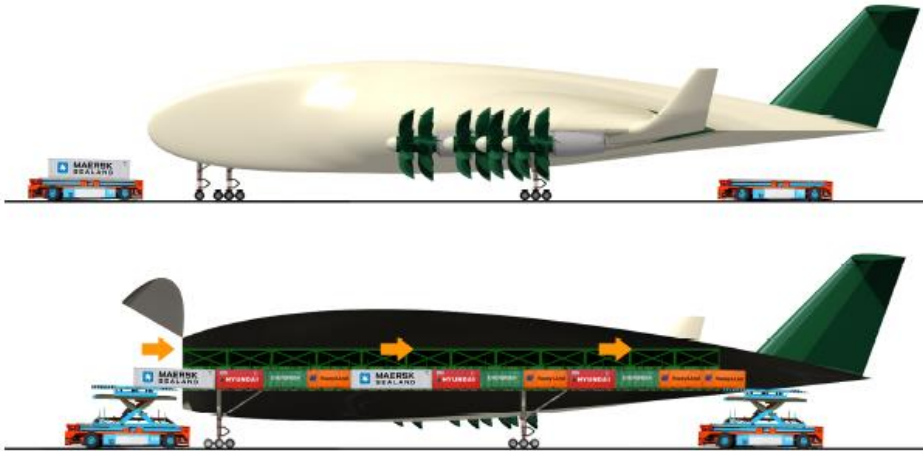


Figure 3. Recent Proposed LH₂ Powerd Aircraft. A liquid hydrogen powered design concept side view presented in 2012 by Delft University.

Table 1. HUULC Aircraft Data. General sizing and performance data presented for the Delft's HUULC aircraft design.⁶

Parameter	Value
W_e	701,000
W_f	141,000
W_{tfo}	2,100
W_{pay}	1,248,000
W_{to}	2,092,000
W/S [N/m^2]	2867
W/P [N/W]	0.065
S [m^2]	7160
P [MW]	316
b [m]	200.1
$C_{L_{max}}$ clean [-]	1.6
$C_{L_{max}}$ takeoff [-]	1.7
$C_{L_{max}}$ landing [-]	1.75
A [-]	5.59
e [-]	0.77

In the case of the hydrogen powered aircraft it would be necessary to not only implement complex cryogenic fluid handling systems in the aircraft (assuming vapor cooling permitted, without this a complex refrigeration system would also be required) but also require that facilities at all potential destinations maintain supplies of cryogenic liquid hydrogen and all the attendant refrigeration and handling equipment. A potential design was presented in the mid 70's that yielded decent overall characteristics except for cargo volume. However, without compelling performance increases over traditional designs and the additional complexity, nothing was ever done with the design.

More recently, a potential hydrogen powered aircraft design was presented by Delft University in 2012⁶. This design utilizes several non-conventional features including a hybrid flying wing – lifting body design, liquid hydrogen powered propulsion, extreme wingspan and dedicated airports. For reasons of logistical integration with the current military airlift network such compromises are unacceptable for a C-5 Galaxy replacement.

In the case of nuclear powered propulsion there are several obvious concerns making such a system prohibitively complex. The foremost concern from a purely aircraft design perspective is that a nuclear reactor, even one designed for aircraft, would be extremely heavy and additional shielding would be required to make sure that any crew, passengers, and sensitive cargo would also be safe from

radiation exposure. Operational concerns involve the fallout in the case of a crash, security of nuclear materials and technology in the case of aircraft loss and provisions for refueling and maintaining a nuclear-powered aircraft.⁵ The weight concern can be seen in the following figure from reference 5 showing the extreme size and extremely poor

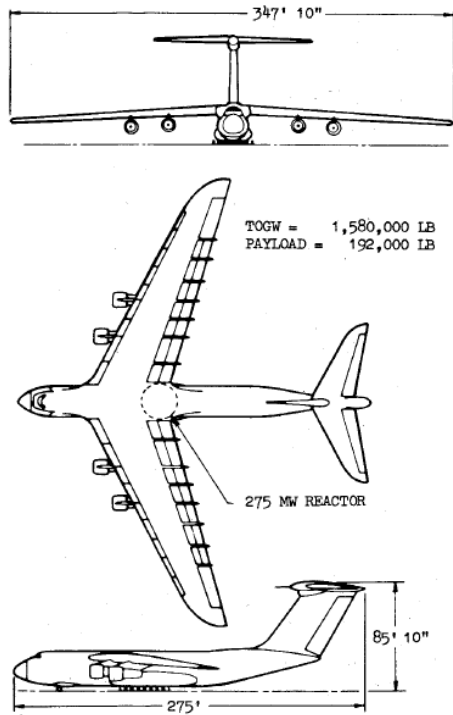


Figure 4. Nuclear Powered Aircraft Concept.
Potential nuclear powered aircraft design evaluated (theoretically) in the mid 70's.⁵

cargo to overall weight ratio of the aircraft design. The most compelling piece of research on next generation military transports that was located was published in 2003 for the RTO-Symposium on Unconventional Vehicles and Emerging Technologies. This paper, written by Wolfgang Heinze and Martin Hepperle⁷ compares a pair of flying wing designs with a conventional design to evaluate the benefits in a comparable manner. Their results show a significant improvement over the conventional design for the flying wing however even their design for the flying wing is only marginally better than the preliminary design thus far conducted for the Goliath. A selection of their results is shown below in table form.

The proposed gross takeoff weight of the smaller flying wing is almost identical to that of the Goliath at this stage of the design process. The Goliath is approximately 5 tons lighter than their proposed design while carrying 20 less tons of cargo over approximately 3000 fewer kilometers. These decreases are significant but not of the same magnitude as predicted by their conventional design case.

From these research cases the trend is clear. New designs for large cargo aircraft are focusing almost exclusively on varying degrees of unconventional designs. This trend has the goal of reaching a similar or higher performance envelope to that of current aircraft for reduced size, weight and cost. However, as has been proven time and time again, unconventional designs historically take more time and money than anticipated and yield less performance than predicted. The most notable case of this is the F-35 Lightning II, which, while a remarkable aircraft, has fallen well short of its initial performance promises and well over-budget.

Table 2. Heinze and Hepperle Data Summary. *Summary of design data from the work of Heinze and Hepperle⁷ on unconventional aircraft design.*

parameter		conventional	flying wing	unit	
<i>mission</i>					
range	R	10'900	10'900	20'000	km
payload	m _{payload}	150'000	150'000	150'000	kg
lift over drag	L/D _{cruise}	18.5	19.7	22.3	-
<i>dimensions</i>					
overall length	l	86.5	50.0	50.0	m
overall span	b	75.5	69.5	82.9	m
overall height	h	24.9	14.3	14.9	m
payload volume		1'938	1'315	1'315	m ³
max. fuel volume		533	926	1'172	m ³
lifting area		813	1'354	1'554	m ²
outboard wing area		n.a.	800	1'000	m ²
aspect ratio	Λ	7.0	6.04	6.87	-
sweep angle	$\Phi_{0.25}$	25	38	35	°
<i>mass</i>					
overall empty	m _{OE}	266'554	164'821	222'291	kg
required fuel	m _{fuel}	218'715	152'904	330'456	kg
max. takeoff	m _{MTO}	635'269	467'725	702'747	kg

IV. Mission Specifications

The mission specification for the proposed aircraft design, the Goliath, represents a significant improvement in payload mass, range, cruise speed, and operational costs over the C5-B and C-5M aircraft currently in operation.

Table 3. Aircraft Specifications. Comparison of C5-M and Goliath Specifications

SPECIFICATION	C5-M ²	GOLIATH
MAXIMUM PAYLOAD (KG)	122472	130000
CRUISE SPEED (KMPH)	833	900
CRUISE ALTITUDE (M)	10600	10700
TAKEOFF ROLL (M)	2600	2600
LANDING ROLL (M)	1100	1400
RANGE*	8056	8000
*C5-M STATED RANGE AT 54431 KG, GOLIATH AT 120000 KG		

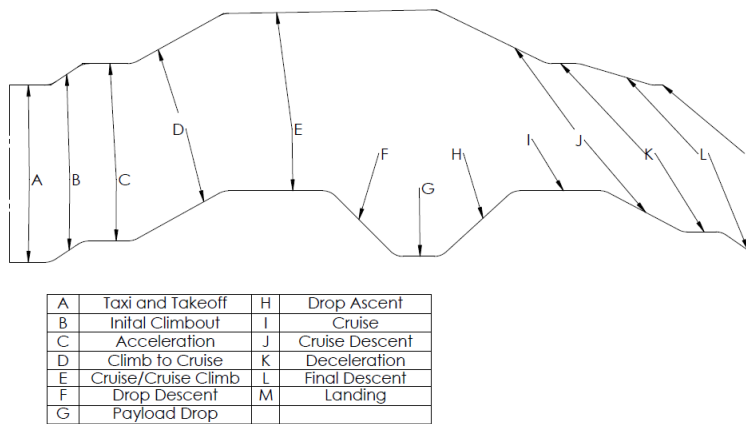


Figure 5. Mission Profile. Breakdown of the design mission profile for the Goliath including contingency options.

with contingencies for missed approach and diversion to alternate landing sites. A diagram of this flight profile is shown in figure 5. The affect of this flight profile on aircraft design will be discussed further in section 4.

V. Class I Design Overview

A. Configuration

The configuration for the Goliath was chosen based primarily upon the desire to reduce cost in development, aquisition and operation. Due to the necessities of the cargo transport mission as well as to enable the use of conventional design and manufacturing techniques in addition to infastructure, a conventional fuselage-wing-tail design was selected that incorporates an aft mounted T-tail, aft-swept high wing, two wing slung high bypass turbofan engines and fuselage mounted landing gear. It can be seen from table 4 below that the only unusual characteristic of this configuration is the number of engines. This will be covered in the weight and performance sizing section. This choice of engine count as well as the typical configuration allows ready application of existing techniques and knowledge to shorten the design process and make it easier to operate and maintain the aircraft, supporting the mission goal of reduced operational cost while reducing the development time and aquisition cost.

While many of the specifications of the two aircraft are similar, there are several important distinctions in the specifications. The modest increase in maximum payload capacity ensures that there is sufficient margin to safely accommodate two battle-ready MBTs with the potential for secondary equipment and supplies to be included. The cruise velocity increase of 8% corresponds to a cruise mach increase of 0.08 from mach 0.77 to 0.85 at the design cruise altitude. This allows the Goliath to arrive 45 minutes sooner than the C5-M over its full payload operational range. Finally, the operational range figure is misleading for the C-5, the operational range of the C-5M is rated at 120000 lb of cargo not its full rated payload capacity. At maximum payload capacity, the estimated range for the C-5M is approximately 3500 km while the Goliath's range remains at 8000 km. This estimation was performed using the Brequet range equation, utilizing the ratio of C-5M's maximum operational weight and the sum of payload and empty operating weight as the mass fraction with all other values assumed to be similar.

The primary mission profile of the Goliath is the same as the C-5M in the form of a point to point cargo mission

Table 4. Aircraft Configuration Comparisons. *Comparison of cargo aircraft with a similar mission profile.*

Designation	Tail	Wing	Gear	Engine	Fuselage	General
An-124	S	AS,HW	Rec,Tri, Fus	Nac,BW,4,HPTF	Conv.	Conv.
C-5	T	AS,HW	Rec,Tri, Fus	Nac,BW,4,HPTF	Conv.	Conv.
C-17	T	AS,HW	Rec,Tri, Fus	Nac,BW,4,HPTF	Conv.	Conv.
IL-76	T	AS,HW	Rec,Tri, Fus	Nac,BW,4,HPTF	Conv.	Conv.
A400	T	AS,HW	Rec,Tri, Fus	Nac,BW,4,HPTF	Conv.	Conv.
AS= Aft-Swept	HW= High Wing	Rec= Retractable	Tri= Tricycle Gear	Fus= Fuselage Mounted Gear	Nac= Nacelle Housing	BW= Below Wing

The performance gains over previous designs, despite utilizing largely the same configuration and mission profile, are obtained by leveraging modern design techniques, removal of extraneous and rarely utilized features, and utilizing modern engine technology to reduce the number of engines to two.

B. Weight Sizing and Sensitivities

Preliminary weight estimations were made by using a historical statistical basis as described in Roskam’s Airplane Design Part I.¹ The aircraft used for this analysis are shown in table 3 below. The choice of aircraft naturally includes most of the military cargo aircraft developed to date as well as some of the heaviest aircraft from the civilian airline market, with emphasis on those aircraft possessing freighter variants.

Using the statistical trends and class one estimations for aircraft weight fractions as well as the Brequet range equation the empty weight and fuel fraction breakdowns have been estimated giving a MTOW of 465t, a empty weight of 200t and a corresponding fuel fraction of 135t. The fuel use for each mission segment is shown below in table 5.

Table 5. Mission Fuel Use Breakdown. *Segment-wise breakdown of the fuel use across all mission segments for the Goliath.*

Mission Segment	Starting Weight (kg)	Used Fuel Weight (kg)	Starting Fuel Weight (kg)
Warmup	471881	4719	139315
Taxi	467162	4672	134597
Take-off	462490	2312	129925
Climb	460178	3502	127613
Cruise	456676	101016	124111
Loiter	355660	7816	23094
Descent	347843	5218	15278
Land/Taxi	342626	3426	10060

Using the method described in Roskam’s Airplane Design Part 1¹ the weight sensitivity characteristics can be calculated. These same methods are implemented in the Advanced Aircraft Analysis software¹⁰ and this software was used to confirm manual calculations.

Table 6. Weight Sensitivity Summary.
*Summary of weight sensitivities for the Goliath. Cj measured in kg/(N*hr).*

$\frac{\partial W_{TO}}{\partial W_{PL}}$	3.1	kg/kg
$\frac{\partial W_{TO}}{\partial W_E}$	2.66	kg/kg
$\frac{\partial W_{TO}}{\partial C_j}$	617508	kg/cj
$\frac{\partial W_{TO}}{\partial R}$	340	kg/km
$\frac{\partial W_{TO}}{\partial \left(\frac{L}{D}\right)}$	-17251	kg/(L/D)

The sensitivities show how much the design takeoff weight may shift based on changes to the preliminary design characteristics. The sensitivity to specific fuel consumption is clearly the dominate factor however changes in specific fuel consumption are likely to be very small (on the order of 0.01). Thus, the primary sensitivities of concern are the sensitivity to thrust specific fuel consumption and the sensitivity to lift to drag. These are also the quantities of greatest uncertainty at this stage of the design process.

C. Performance Analysis

The primary performance for this design were calculated using the method described in Roskam.¹ This method produces several curves represented as thrust to weight ratio vs wing loading. These curves restrict the design point of the aircraft to having a thrust to weight ratio higher than all of the curves dependent on thrust to weight ratio and to have a wing loading that is lighter than those curves dependent on wing loading. These curves were assembled into a matching graph which was used to determine the design point of the aircraft. As a result of these constraints, the wing loading required at the desired design point is 5500 N/m² with a thrust to weight ratio of 0.26. Combining these values with the projected maximum takeoff weight determined that the wing area required for the aircraft is 840 square

meters of projected wing area and 1.2MN of thrust required. The wing area is similar to that of an A380⁸ which is reasonable based upon the lower takeoff weight but more stringent takeoff and landing requirements. The thrust requirement presents more of an issue as it requires a thrust per engine of 600kN, 20% higher than the existing GE90-115B certified thrust, currently the most powerful aircraft certified jet engine.⁹ For such a lengthy major design project it is reasonable to assume that the progression of turbofan engine development in parallel with aircraft development will result in an acceptably powerful jet engine at the point of aircraft integration.

The primary reason for selecting a two engine design is one of cost. Two engines cost less to acquire and maintain than four engines. Additionally, the increased reliability of today's turbofan engines reduce the likelihood of failure to a level that is acceptable for use in a critical infrastructure link such as the proposed Goliath. There is an intermediate option between the two and four wing mounted engine configurations in the form of two wing mounted engines with an additional engine mounted in the tail. However, due to the presence of a rear cargo door and its attendant hydraulics, and structural components, utilizing a three engine design with one of the engines in the tail of the aircraft was not found to be a feasible design choice.

The thrust required and wing loading dominate the remainder of the aircraft design.

D. Fuselage Design

The fuselage design of the Goliath incorporates both a nose and tail cargo access door similar to other large military transports to facilitate rapid loading and unloading of regular and oversize cargo. The ability to rapidly load and unload the aircraft is important due to the militarily important nature of the cargo as well as the potentially dangerous locations where the loading and unloading operations are taking place. While there are bump fairings, the landing gear also needs appropriate volume to retract into fuselage to avoid excessively large fairings. The other major defining features for the fuselage are the flight deck and upper level compartment which require certain sight lines for the cockpit and minimum height for the upper compartment such that a person can stand unobstructed. The fuselage has interior volume for a flightdeck, upper compartment, measuring approximately 6 x 2x 30 meters (partially interrupted by primary wing structure), the primary cargo compartment, measuring approximately 5 x 5 x40 meters, and the fore and aft loading ramps.

E. Wing Design

The wing design for the Goliath was principally based on two characteristics in addition to the required wing area determined in the performance constraint step of the design process. The wing thickness and wing sweep angle are the primary factors in determining the critical mach number of the aircraft. A trade study was conducted that relates the wing thickness and sweep angle to the weight of the wing structure with the goal of satisfying the critical mach number requirement. The results of this can be seen in part below in figure 4. The preliminary design decision was to

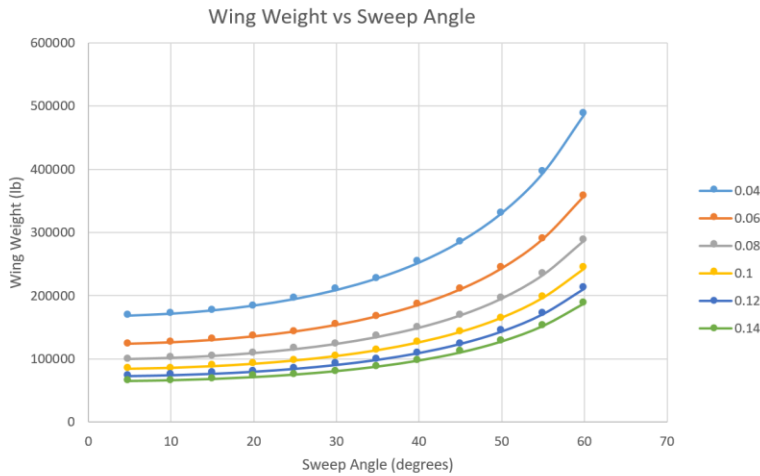


Figure 6. Wing Sweep and Thickness Trade Study. Shows the relation of wing sweep and thickness (shown relative to chord by separate lines) to the weight of the wing structure. The relation was defined in Roskam utilizing pounds and the calculation used the same,

utilize a wing that is 12% thick with a quarter chord sweep angle of 25 degrees which minimizes weight while attaining the required critical mach number. This resulted in a wing with an estimated weight of approximately 40 t.

Other design values for the wing were chosen as preliminary values from historical data and reasonable ranges for similar types of aircraft. The wing design at this stage has 25 degrees of sweep, 12% thickness, four degrees of anhedral, a taper ratio of 0.38. The choice of airfoil for this wing is the Sellig SG6043 which couples the required levels of $C_{L_{max}}$ with a high lift to drag ratio.

The high lift devices, slats and flaps, as well as ailerons were sized per Roskam⁵ to attain, respectively, the required $C_{L_{max}}$ for the wing and roll authority. The wing has a total

resultant span of 90 meters and, as shown in figure 5, a root chord of 14 meters, tip chord of 4.2 meters and mean aerodynamic chord of ~10 meters.

F. Emmpenage Design

The emmpenage of the Goliath is, as previously discussed, a T-tail style emmpenage. This helps make the tail smaller by increasing the moment arm of the horizontal stabilizer and increasing the effective aspect ratio of the vertical stabilizer. The tail sizing has been determined with the volume fraction method with other geometric parameters being based on typical values for similar aircraft. The volume fraction method is calculated in equation 1 and 2 as shown below.

$$\bar{V}_h = \frac{x_h * S_h}{S * \bar{c}} \rightarrow S_h = \frac{(\bar{V}_h * S * \bar{c})}{x_h} = \frac{0.6 * 840 m^2 * 10 m}{45 m} = 112 m^2 \quad (1)$$

$$\bar{V}_v = \frac{x_v * S_v}{S * b} \rightarrow S_v = \frac{(\bar{V}_v * S * b)}{x_v} = \frac{0.08 * 840 m^2 * 92 m}{40 m} = 154.56 m^2 \quad (2)$$

Using the above surface area we can determine the other geometric characteristics that define the stabilizers. The vertical stabilizer has a sweep angle of 30 degrees, a constant chord of 11.75m. The thickness of the tail is 10% utilizing a NACA 0010 airfoil. The rudder makes up the aft 35% of the vertical stabilizer. The vertical stabilizer design can be seen as a side projection in figure 6 below.

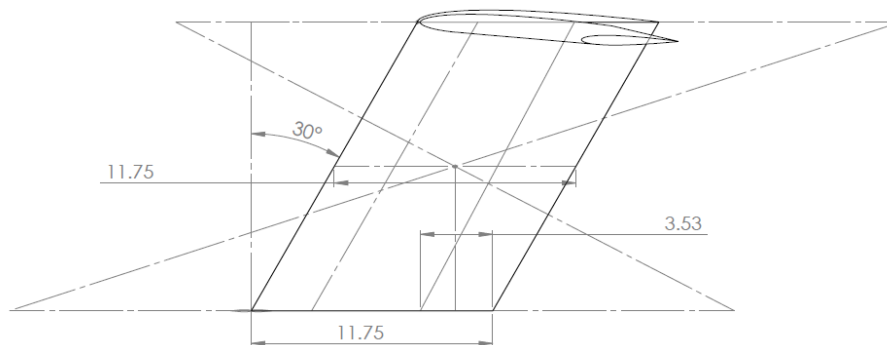


Figure 7. Side View of the Vertical Stabilizer. Geometric breakdown of the vertical stabilizer.

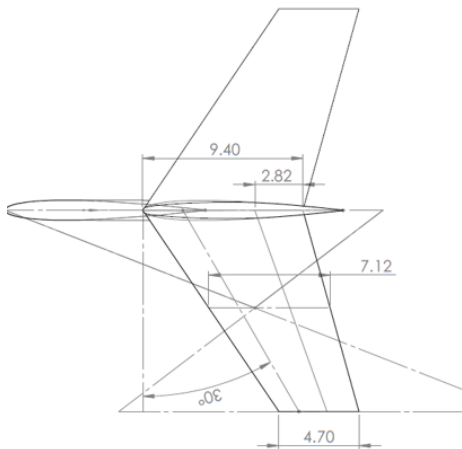


Figure 8. Planform View of the Horizontal Tail.
Geometric layout of the horizontal tail.

The horizontal stabilizer has a taper ratio of 0.5 with the same sweep angle as the vertical stabilizer of 30 degrees. The horizontal stabilizer has a root chord of 9.4 meters with a mean aerodynamic chord of 7.1 meters and a full span of 23.6 meters. The elevator is a constant chord elevator that spans the trailing 2.8 meters. While not the ideal choice aerodynamically the horizontal stabilizer also utilizes a NACA 0010 airfoil for simplicity of manufacturing and commonality with the vertical stabilizer.

G. Landing Gear

The landing gear is the last major component to be discussed. The primary concerns for the landing gear are the feasibility of retraction into the fuselage, the lateral stability and longitudinal stability. For the longitudinal stability the line between the center of mass of the aircraft (projected) and the rear main tires should be 15 degrees off of vertical with the rear wheels aft of the center of

gravity. For lateral stability, a line is drawn from the center of the nose gear to the outside of the rear landing gear (either side). The line that is perpendicular to this line and coincident to the center of mass must be less than 55 degrees out of the horizontal plane. The preliminary placement of the landing gear is made to satisfy this requirement as shown in figure 9.

The landing gear placement has been verified to be acceptable at all loading scenarios including no payload, fuel but no payload and fully loaded states. The gear position has been additionally verified to be compatible with the available volume in the fuselage for retraction for both the forward and the aft landing gear. A preliminary design for

the landing gear boogies, common between the forward and main gear arrangements, is shown in figure 12.

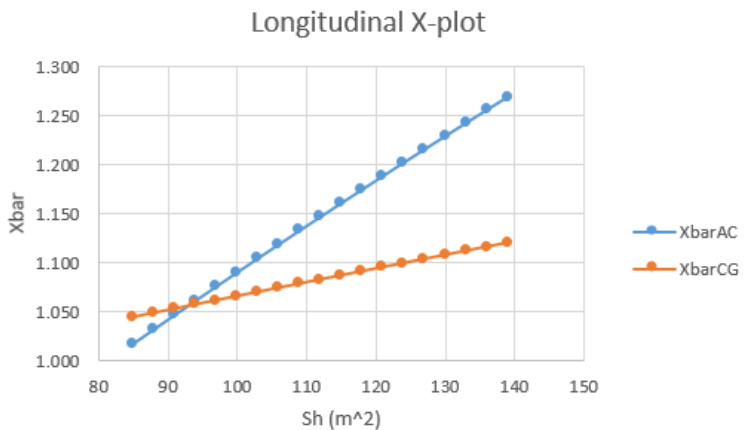


Figure 9. Longitudinal X-plot. *Plot to verify the sizing of the horizontal stabilizer with respect to the initial sizing estimate.*

H. Stability and Control

Verification of the stability and control of the aircraft is important to ensure that the aircraft is stable and controllable. A x-plot for the horizontal stabilizer is presented in figure 12 (left). A plot is also present for the lateral stability however the lateral stability and control criteria is dominated by the ability to control the aircraft in the event of an engine failure. Ensuring sufficient control in this

condition can be done by making sure the required rudder deflection at stall speed is an acceptable value. This is shown in equation 3 below.

$$\delta_r = \frac{(N_D + N_{t_{crit}})}{\bar{q}_{mc} * S * b * C_{n_{\delta_r}}} = \frac{15E6}{(0.5 * 1.09 * 75^2 * 840 * 92 * 0.0025)} = 25 \text{ deg} \quad (3)$$

The rudder size is acceptable since deflection required from the rudder, while admittedly large, is within the range of reasonable rudder deflections.

VI. Class I Reevaluation

There were several known major outstanding issues remaining from the class I design process for the Goliath. While manageable in the long term, these issues were addressed here to ease the difficulty of addressing them later in the design process should they become more serious. A fourth issue came to light during the process of resolving these issues which will also be discussed.

Table 7. Weight Sensitivity Summary.
*Summary of weight sensitivities for the Goliath. C_j measured in kg/(N*hr)*

$\frac{\partial W_{TO}}{\partial W_{PL}}$	3.1	kg/kg
$\frac{\partial W_{TO}}{\partial W_E}$	2.66	kg/kg
$\frac{\partial W_{TO}}{\partial C_j}$	617508	kg/cj
$\frac{\partial W_{TO}}{\partial R}$	340	kg/km
$\frac{\partial W_{TO}}{\partial \left(\frac{L}{D}\right)}$	-17251	kg/(L/D)

straightforward one when coupled with the previously changed wing sweep angle. The increased wing sweep moves the center of lift aft and moving the entire wing back moves both the center of mass and center of lift back allowing the desired static margin to be maintained while allowing a sufficient rotation angle for the aircraft. The main gear and its attendant housing was moved 3 meters aft to accomplish this with a smaller one meter rearward move for the wing.

The fourth issue was an excessively large wingspan. The Goliath initial wingspan for its given aspect ratio was 91.6 meters, approximately 12 more than the Airbus A380⁸ and beyond the Group V classification (FAA and ICAO) for aircraft size¹¹, demanding a wider runway and taxiways than other aircraft as well as increased spacing. Reducing the aspect ratio from 10 to 7.5 brought the wingspan down to 79.376 m, with the range of Group V classification. This change would naturally also reduce the L/D ratio of the aircraft, exacerbating the weight increase due to weight sensitivities, however, the final change prior to class II aircraft design steps reversed this decrease.

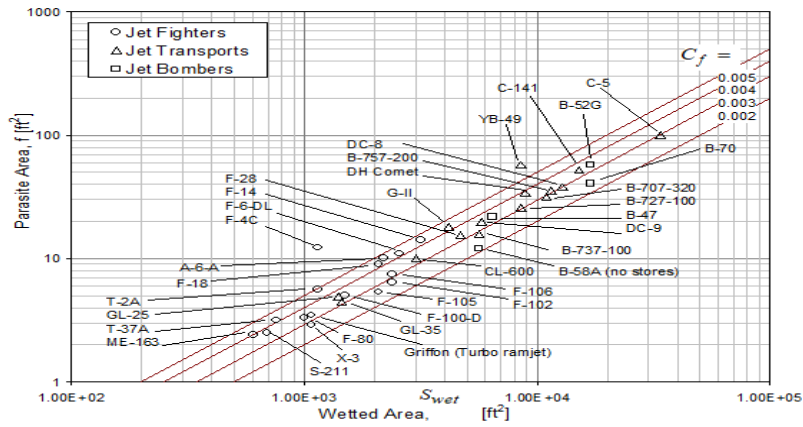
The final change to the aircraft is an analytical rather than design one. In order to construct the class I drag polars for the aircraft a skin friction coefficient had to be chosen. At this stage of the design process it is necessary to assume a value based on previous aircraft designs. The previously chosen value was chosen in error as 0.006 when based on historical data for the C-5 Galaxy and other aircraft the value should have been 0.003. The skin friction coefficient naturally has a great effect on the drag of any well designed aircraft as the majority of the drag of a “clean” aerodynamic body is skin friction drag with pressure drag being small by comparison. The historical trends for aircraft C_f can be seen in figure 10 below.

The first issue was a lower than anticipated L/D. The projected L/D for the aircraft in the early design stages was assumed to be 16. This value is at the high end of the expected range for large cargo aircraft.¹ In the later stages of class I design it was determined that the L/D for the Goliath was 15.7 during cruise. While this value is only slightly different than the projected value it was necessary to use the previously determined weight sensitivities to adjust the MTOW of the aircraft upwards by 5.2 tons (1.1%). For reference the full range of weight sensitivities can be found in table 6.

The second issue was an incorrect wing sweep angle. The wing sweep angle originally selected (25 degrees relative to quarter chord), was insufficient to provide a drag divergence mach number allowing efficient cruising at the desired speed of mach 0.85. The solution to this problem was to increase the wing sweep from 25 to 30 degrees. This new angle provides a sufficiently high drag divergence mach number for efficient cruising with the penalty of slightly increasing the wing structure weight. From previously conducted trade studies the wing structural weight increase is approximately 7%.

The next issue was the main landing gear placement. The gear as placed during the preliminary design would have severely limited the rotation angle of the aircraft on the takeoff roll. This is a critical problem for aircraft of any class. However the solution is a

Combining these changes of aspect ratio and C_f the new L/D ratio for the aircraft was determined by reevaluating the drag polars. These reevaluated drag polars as well as the cruise condition are shown below in figure 11. The new L/D after reviewing these issues was determined to be 19 for the Goliath.



Parasite Area vs Wetted Area for Fighters, Bombers, Transport

Figure 10. Historic Skin Friction Coefficients. Plot showing the skin friction coefficient of various previous aircraft. For the purposes of designing the Goliath, the C-5 is of particular note.¹

This necessitated some recalculation of critical values due to the significant difference between this value and the original assumed value for the lift to drag ratio. The recalculations were time consuming but straightforward, being a simple reassessment of steps discussed in previous reports and will not be discussed further here. The updated design three view can be seen in figure

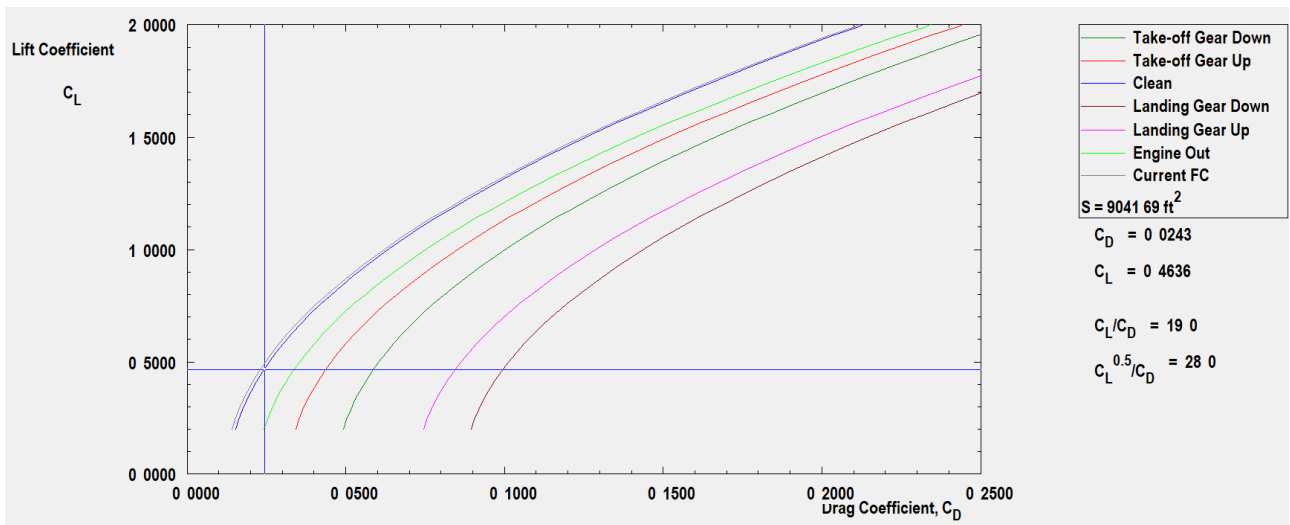


Figure 11. Class I Drag Polars. Revised drag polars to account for adjusted aspect ratio and skin friction coefficient.

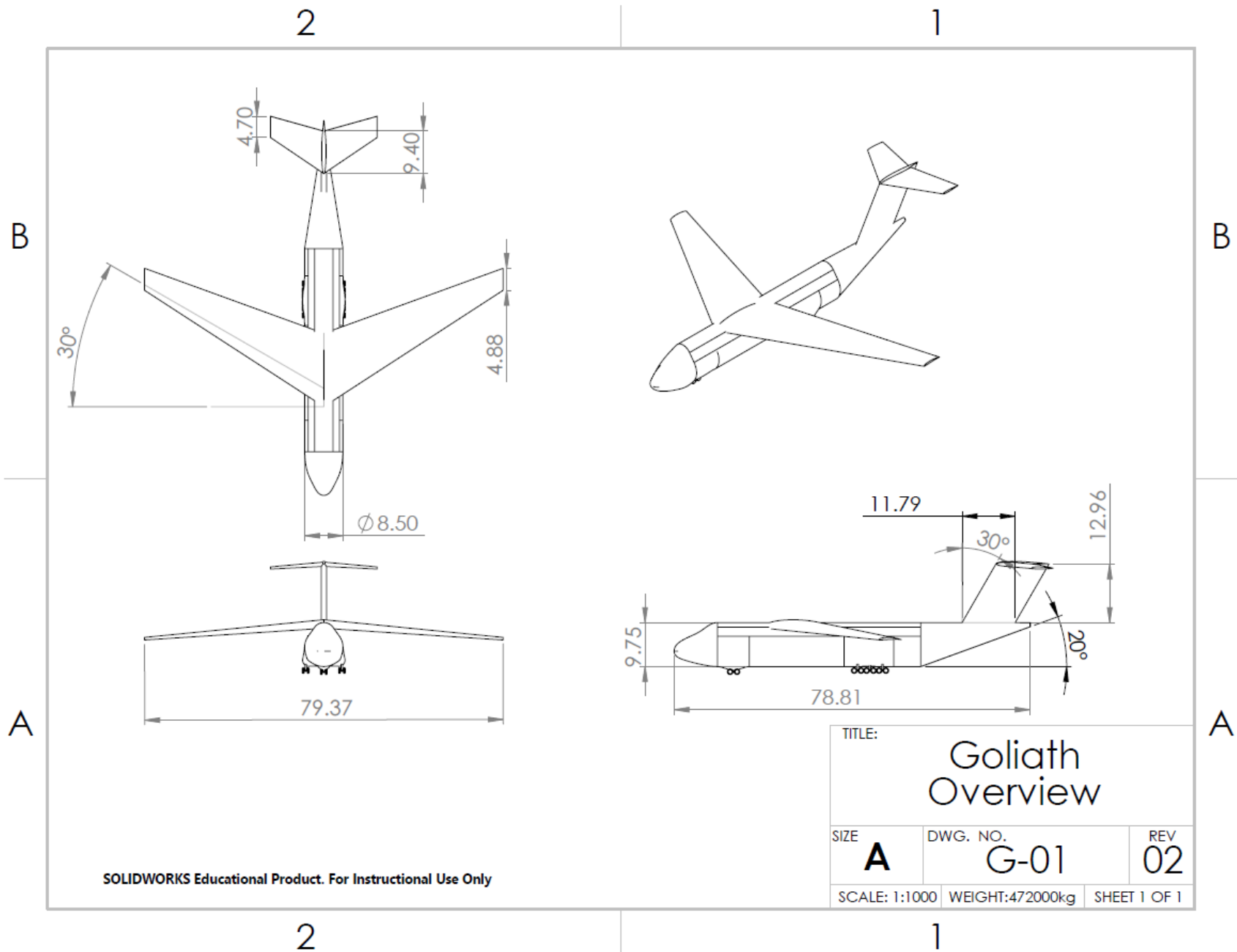


Figure 12. Revised Aircraft Geometry. Revised aircraft geometry to reflect class I reevaluation.

VII. Class II Landing Gear and Tire Design

With the revision of the aircraft to resolve the major outstanding issues, class II design can commence. The first step in the class II design conducted was the class II landing gear configuration. The preliminary gear configuration has been selected in class I design and these class II steps will serve to determine the true strut and tire size. The first step in this procedure is to calculate the equivalent single wheel load (ESWL). This can be calculated for the given strut configuration as $ESWL=P/2$ where P is the per strut load on the gear (applicable to both main and nose gear). From geometric layout of the aircraft the load distribution between the main and nose gear can be calculated based on a simple ratio of the respective distance from the center of mass (calculated with rearmost CG for main gear and most forward for nose gear). This ratio can be found to be 24:5 (meters) for the (respectively) nose and main gear spacing from the CG in nominal position. Taking the extreme CG positions, it can be calculated that the nose gear loads are a maximum of 18% of the MTOW and the main gear loads are 85% of the MTOW. Knowing that there are two nose gear struts and eight main gear struts (from class I design) we can calculate the ESWL for the nose gear.

$$ESWL_n = 0.18 * 1.04 * 106 \frac{lb}{2 * 2} = 46800 \text{ lb} \quad (4)$$

$$ESWL_m = 0.85 * 1.04 * \frac{106}{2 * 8} = 55250 \text{ lb} \quad (5)$$

Knowing the ESWL for each gear section and the maximum tire pressure for rough fields of 60 PSI we can see from Roskam's Airplane Design volume 4 that the landing classification number (LCN) for this aircraft is 40 (based on the higher value for the main gear).

Knowing the load per strut and the number of tires per strut it is now necessary to size the tires for the nose and main gear carriages. In order to calculate the tire size we must establish a dynamic load factor to assess dynamic loads that are necessarily greater than static loads. From Roskam we have that all new tire designs utilize a dynamic load factor of 1.5 times the static load. Determining the maximum static load is simple from the previously determined ESWL. The ESWL can be divided by the number of wheels per strut to yield the maximum static load per tire.

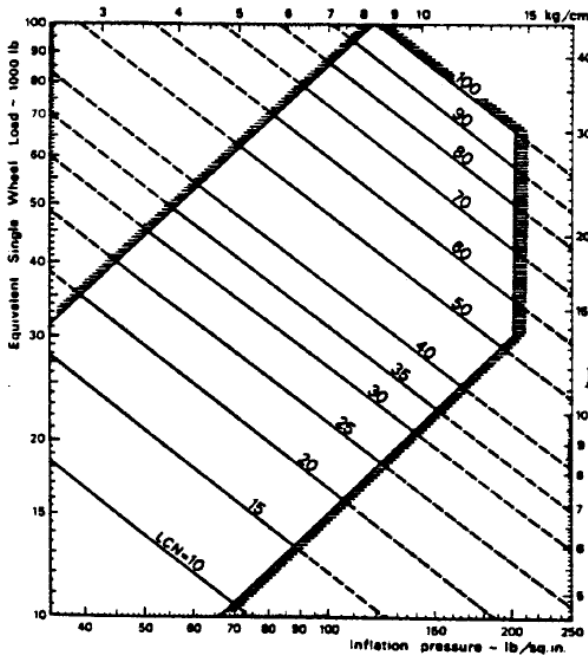


Figure 13. ESWL and LCN Graph. Graph showing the LCN for a given ESWL and tire pressure

$$P_{n,stat} = \frac{46800}{4} = 11700 \text{ lb} \quad (6)$$

$$P_{m,stat} = \frac{55250}{4} = 13812 \text{ lb} \quad (7)$$

Determining the dynamic tire loading is more complex and involves a number of factors. The formulation of this problem is given by Roskam to be:

$$P_{n,dynam} = MTOW * \frac{l_m + \left(\frac{a_x}{g}\right) * h_{cg}}{n_t * (l_m + l_n)} = 1.06 * 10^6 * \frac{5 + 0.4 * 20.5}{(8 * (5 + 24))} = 60310 \text{ lb} \quad (8)$$

$$P_{m_{dynam}} = MTOW * \frac{l_n + \left(\frac{a_x}{g}\right) * h_{cg}}{n_t * (l_m + l_n)} = 1.06 * 10^6 * (24 + 0.4 * 20.5) / (32 * (5 + 24)) = 36780.172 \text{ lb} \quad (9)$$

Utilizing the dynamic load factor, the dynamic loads divided by the dynamic load factor should be used rather than the previously calculated values to ensure tire performance. Consulting the Goodyear Aviation tire selection, the tire that meet this performance specification are 50 inches in diameter and 20 inches wide (50x20.0R22 P34).

With the tire sizing complete it is necessary to size the struts for the landing gear. This can be done by utilizing equation 2.13 from Roskam relating the strut diameter to the static load.

$$D_s = 0.041 + 0.0025 * p_m^{0.5} = 0.041 + 0.0025 * \left(0.85 * 1.06 * \frac{10^6}{8}\right)^{0.5} = 0.90 \text{ ft} \quad (10)$$

$$D_s = 0.041 + 0.0025 * p_n^{0.5} = 0.041 + 0.0025 * \left(0.18 * 1.06 * \frac{10^6}{2}\right)^{0.5} = 0.82 \text{ ft} \quad (11)$$

This concludes the sizing of the landing gear tire and struts. Brake properties are to be evaluated separately.

VIII. Preliminary Structural Arrangement

Preliminary structural arrangements were made in the form of frame, spar, and longeron spacing for the fuselage, wing, and empennage. These spacings were determined using a historical basis from aircraft of a similar scalar.

The torque box for the wing is constructed of a pair of spars located at 15 and 65% of the wing's chord respectively and supplementary stringers spaced at 18 inches between these spars. The position of the front and rear spar places them just aft and forward of high lift devices for the front and rear spar respectively. Wing ribs are placed every 24 inches along the span of the wing with much larger structural ribs located at the engine mount to help distribute its load into the primary wing structure.

The fuselage has frames spaced 22 inches apart with longerons 12 inches apart. Longitudinal beams run through the subfloor between the secondary and primary cargo compartments as well as below the primary cargo bay floor to support the primary cargo. Primary conduits run between the cargo compartments along the long axis of the aircraft. The nose door utilizes fewer supports since it does not need to transmit structural loads and to lighten the door for the purposes of easing actuation. Additional support frames are included at the landing gear attachment points and wing box to reinforce these structurally critical interfaces.

The empennage of the aircraft utilizes a similar spacing to the wings, with main and secondary spars located at 10% and 65% chord respectively. Ribs are spaced every 24 inches apart. No special considerations were needed for the empennage because there are no additional components mounted to the empennage.

A full page presentation of the previously shown 3-view is presented here for reference, although at this time these structural arrangements are only preliminary.

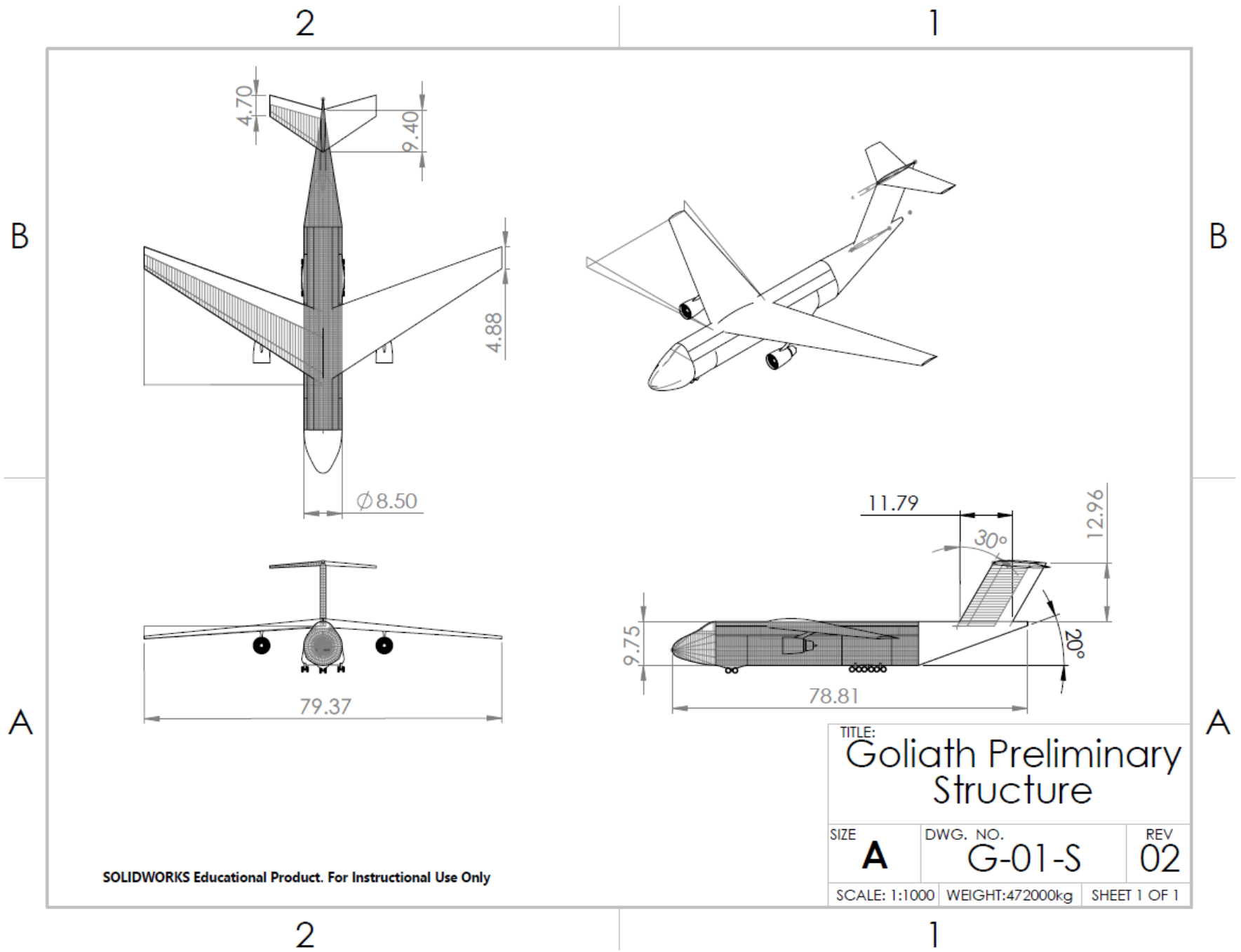


Figure 14. Partial Outline of Preliminary Structural Elements

IX. V-N Diagram

The V-n diagram is based on several critical speed values which are calculated as shown here per Roskam¹.

$$V_{S_1} = \left(\frac{2 * \left(\frac{GW}{S} \right)}{\rho * C_{N_{max}}} \right)^{0.5} = \left(\frac{2 * \left(\frac{1.04 * 10^6}{9041} \right)}{0.00074 * 1.1 * 1.8} \right)^{0.5} = 733.86 \frac{km}{hr} \quad (12)$$

$$C_{N_{max}} = 1.1 * C_{L_{max}} \quad (13)$$

$$V_A = \text{Design maneuvering Speed} \geq V_{S_1} * n_{lim}^{0.5} = 733.86 * 2^{0.5} = 1037.84 \frac{km}{hr} \quad (14)$$

$$V_C = \text{design cruising speed} = 900 \frac{km}{hr} \quad (15)$$

$$V_B = \text{maximum gust loading design speed} = V_C - 79.6 \frac{km}{hr} = 900 - 79.6 = 820.4 \frac{km}{hr} \quad (16)$$

$$V_D = \text{design diving speed} = 1.25 * V_C = 1.25 * 900 = 1125 \frac{km}{hr} \quad (17)$$

The calculation of the V-n diagram is straightforward from these numbers and is presented in detail in Roskam¹ volume 5. The V-n diagram, shown in figure 15, is primarily used to evaluate the aircraft's ultimate load cases which are in turn used for details structural weight estimations using a class II method. These class II weight estimations are in progress but have not been completed to the point of presentable results.

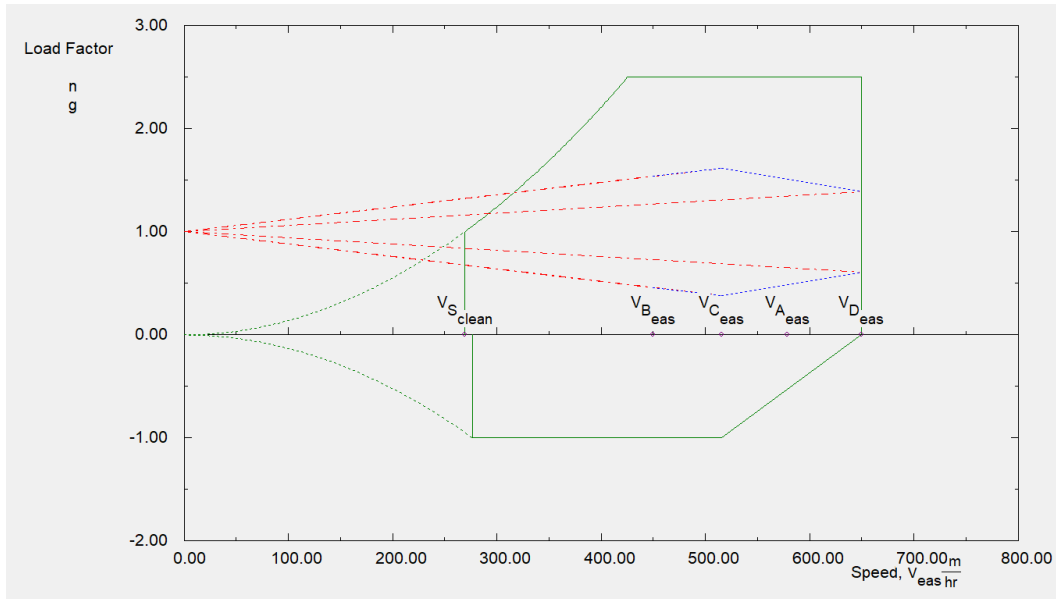


Figure 16. V-n Diagram. Basic V-n diagram for the Goliath.

X. Class II Weight Estimation

Table 8. Class II Structural Component Weights Breakdown of class II weight estimates for all major structural components.

Component	Component Weight(kg)			
	GD	Torenbeek	Vought	Average
Wing	31450.85	60580.8359	49388.48	47140.07
Horizontal	5040.479	3343.18043	3697.472	4027.054
Vertical	2913.884	4393.04791	1942.12	3083.017
Pylon	N/A	N/A	N/A	326.1978
Fuselage	31746.87	N/A	38007.06	34876.97
Landing Gear	10144.75	23889.6534	23907.6	19314.01
TOTAL:				108767.3

Component	Component Weight(lb)			
	GD	Torenbeek	Vought	Average
Wing	69336.54	133556.511	108881.8	103925
Horizontal	11112.24	7370.37557	8151.447	8878.043
Vertical	6423.948	9684.91342	4281.598	6796.82
Pylon	N/A	N/A	N/A	719.1356
Fuselage	69989.15	N/A	83790.37	76889.77
Landing Gear	22365.12	52667.1299	52706.7	42579.66
TOTAL:				239788.4

Class II estimation techniques presented in Roskam¹ were used in this phase of the design process to evaluate rather the layout and other aspects of the design support meeting the weight targets that have been set in the aircraft sizing. Resassment at this stage is necessary to make sure the nearest thing to an optimal design point has been chosen. Should the weight come in below target the aircraft is larger than necessary for its design use-case and if it is more massive then the aircraft must be enlarged and reinforced causing a increasing spiral of weight increases, in either case the design would require iteration to maintain acceptable performace relative to the design intentions on its primary missions.

The process presented here is a overview of the process used since the process used is similar in almost its entirety to that presented in Roskam¹ Vol 5 and implemented in software to support rapid iteration of the design.¹⁰

A. Structure

The methods used here and outlined in Roskam¹ are a collection of equations determined through historical and emperical analysis of aircraft design to provide an approximate matching curve to the trends in aircraft design aspects across a specified range of aircraft. In the case of the Goliath the trends used are obviously for large aircraft that operate in the high subsonic range. Several such trends exist and since they are theoretically equally applicable to a design at this stage, their results are averaged to determine the Class II analysis weight of the structural

components.

These equations vary from structural component to component however a version of these equations for the wing are presented below in equation 18-20.

$$W_{wGD} = \frac{0.00428(S^{0.48})(A)(M_H)^{0.43}(W_{TO} * n_{ult})^{0.84}(\lambda)^{0.14}}{\left(\left(100\left(\frac{t}{c}\right)_m\right)^{0.76}(\cos\left(\Lambda_{\frac{1}{2}}\right))^{0.154}\right)} \quad (18)$$

$$W_{wtorenb} = 0.0017W_{MZF} * \left(\frac{b}{\cos\left(\Lambda_{\frac{1}{2}}\right)}\right)^{0.75} * \left(1 + \left(\frac{6.3 \cos\left(\Lambda_{\frac{1}{2}}\right)}{b}\right)^{0.5}\right) * (n_{ult})^{0.55} * \left(b * \frac{S}{t_r} * M_{MZF} * \cos\left(\Lambda_{\frac{1}{2}}\right)\right)^{0.30} \quad (19)$$

B. Powerplant

Powerplant weight is estimated on a extrapolation of jet engine dry weight vs takeoff thrust. The graph used to make this estimation is presented in figure 16 below.

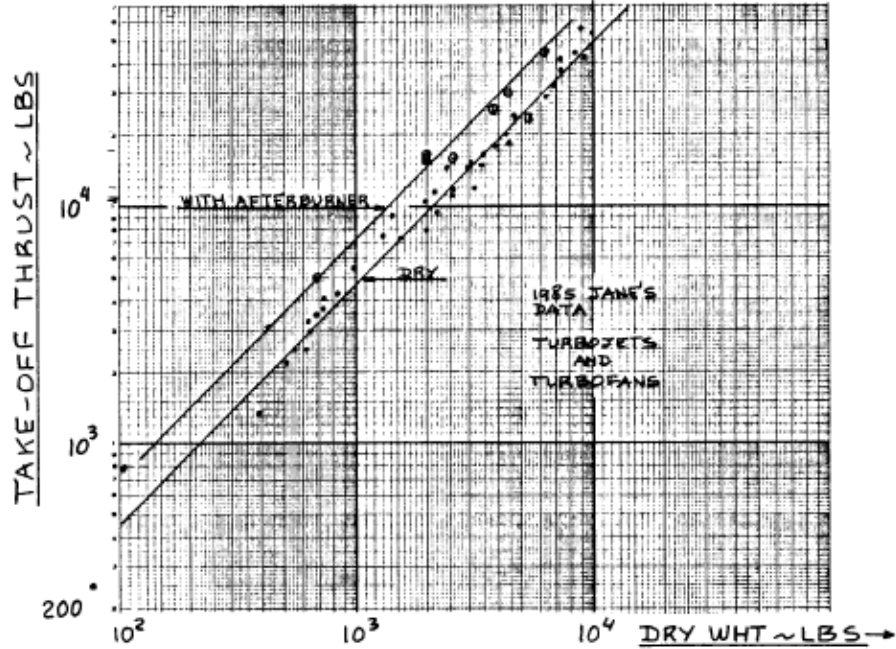


Figure 16. Engine Weight Estimation Trend. Graphical trend for estimating to greater precision the weight of the engines of th Goliath

The required thrust per engine places the engines of the Goliath slightly off of this chart however and a different method needs to be used. Luckily Torenbeek has developed a simiar estimation to those used for structural weight.

$$W_{engTorenB} = \frac{10 * N_{eng} * (32.174 * \dot{m}_a) * \left(\frac{P_{t3}}{P_{t2}}\right)^{0.25}}{1 + BPR} + 0.12 * K_{fan} * T_{total} * \left(1 - \frac{1}{(1 + 0.75 * BPR)^{0.5}}\right)$$

$$= \frac{10 * 2 * (32.174 * 3710) * (42)^{0.25}}{1 + 10} + 0.12 * 1.4 * 1400000 * \left(1 - \frac{1}{(1 + 0.75 * 10)^{0.5}}\right) = 322927.6 N = \mathbf{32929 kg} \quad (20)$$

C. Fixed Equipment

Fixed equipment is broken down into several categories with a similar approach to the structural breakdown. The equations below represent those for the flight control system and similar equations exist for all the fixed equipment categories in varying degrees of complexity (generally as complex or simpler than the equations shown here).

$$W_{fcsGD} = 15.96 * \left(\frac{W_{TO} * \bar{q}_D}{100000}\right)^{0.815} + W_{cg,ctrl} = 15.96 * \left(5227757.2 * \frac{27301.43}{100000}\right)^{0.815} = 72245.8 N = 7367.02 kg$$

$$\bar{q}_D = 0.5 * \rho_{SL} * (1.689 * V_{DiveEAS})^2 = 0.5 * 1.225 * (1.689 * 125)^2 = 27301.43$$

$$W_{cg,ctrl} = 0, No CG control system present \quad (21)$$

Table 9. Class II Fixed Equip. Component Weights Breakdown of class II weight estimates for all major fixed system components.

System	System Weight(kg)			
	GD	Torenbeek	Vought	Result
Flight Control	7367.059	N/A	1019.14	4193.1
Instrumentation/Avionics	4848.775	1557.084	946.7909	2619.94
AC/Pressure/Icing	1739.237	N/A	1716.793	1913.181
Aux Power	N/A	1567.791	1346.032	1613.036
Cargo	65.64966	N/A	2812.29	1593.162
Hydraulics/Pneumatics	N/A	3135.49	248.7101	1873.473
Electrical Systems	1417.341	N/A	845.3287	1252.452
Oxygen Systems	132.7779	240.226	N/A	206.4834
Furnishings	4902.831	N/A	7597.404	6919.86
Operational Items	N/A	2429.864	N/A	2429.864
			TOTAL=	25091.77

System	System Weight(lb)			
	GD	Torenbeek	Vought	Result
Flight Control	16241.58	N/A	2246.819	9244.202
Instrumentation/Avionics	10689.72	3432.783	2087.317	5775.978
AC/Pressure/Icing	3834.361	N/A	3784.88	4217.842
Aux Power	N/A	3456.388	2967.493	3556.136
Cargo	144.7327	N/A	6200.037	3512.32
Hydraulics/Pneumatics	N/A	6912.573	548.3118	4130.301
Electrical Systems	3124.703	N/A	1863.631	2761.185
Oxygen Systems	292.7252	529.6076	N/A	455.2179
Furnishings	10808.89	N/A	16749.41	15255.68
Operational Items	N/A	5356.932	N/A	5356.932
			TOTAL=	55317.89

D. Center of Gravity

In what is practically an accounting exercise, the weights and locations of all of these items have been tabulated and used to calculate the CG of both the empty and loaded aircraft. The table and these results can be found in table 10.

Table 10. Class II Center of Gravity Table *Breakdown of class II weight estimates for all major components and their locations..*

Component	Weight (N)	Weight (kg)	Weight (lb)	Xcg (m)	Ycg (m)	Zcg (m)
Wing	462444.1	47140.0714	103925.0013	40.33	0.00	5.24
Horizontal Tail	39505.4	4027.05403	8878.043307	75.97	0.00	18.81
Vertical Tail	30244.4	3083.01733	6796.820004	71.42	0.00	14.01
Pylon	1600.0	163.098879	359.567788	32.00	-0.00	6.50
Fuselage	342143.1	34876.9725	76889.77352	34.91	0.00	4.37
Nacelle	58227.3	5935.50459	13085.41341	27.94	0.00	4.00
Nose Landing Gear	24979.6	2546.34047	5613.662198	12.00	0.00	3.00
Main Landing Gear	164490.8	16767.6656	36965.99569	41.00	0.00	3.00
Engine	322927.6	32918.2059	72571.47675	26.00	0.00	4.00
Fuel System	5673.6	578.348624	1275.027376	30.00	0.00	6.00
Propulsion System	7336.3	747.83894	1648.685727	30.00	0.00	6.00
Flight Control System	41120.0	4191.64118	9240.892151	45.00	0.00	8.00
Hydraulic and Pneumatic System	18372.4	1872.82365	4128.827017	45.00	0.00	8.00
Instruments/Avionics/Electronics	25692.7	2619.0316	5773.917066	16.00	0.00	8.00
Electrical System	12282.3	1252.01835	2760.199651	45.00	0.00	8.00
Air Cond./Press./Icing System	18761.8	1912.51784	4216.336828	20.00	0.00	8.00
Oxygen System	2024.9	206.411825	455.0555087	18.00	0.00	8.00
Auxiliary Power Unit	15818.4	1612.47706	3554.866936	60.00	0.00	8.00
Furnishings	67860.3	6917.46177	15250.23623	45.00	0.00	4.00
Cargo Handling Equipment	15623.5	1592.60958	3511.067085	45.00	0.00	4.00
Operational Items	23828.7	2429.02141	5355.020593	14.00	0.00	8.00
Other Items	9532.7	971.732926	2142.282408	45.00	0.00	4.00
TOTAL	1710489.9	174361.865	384398.1686	35.71	0	5.16

XI. Reassessed Drag Polars

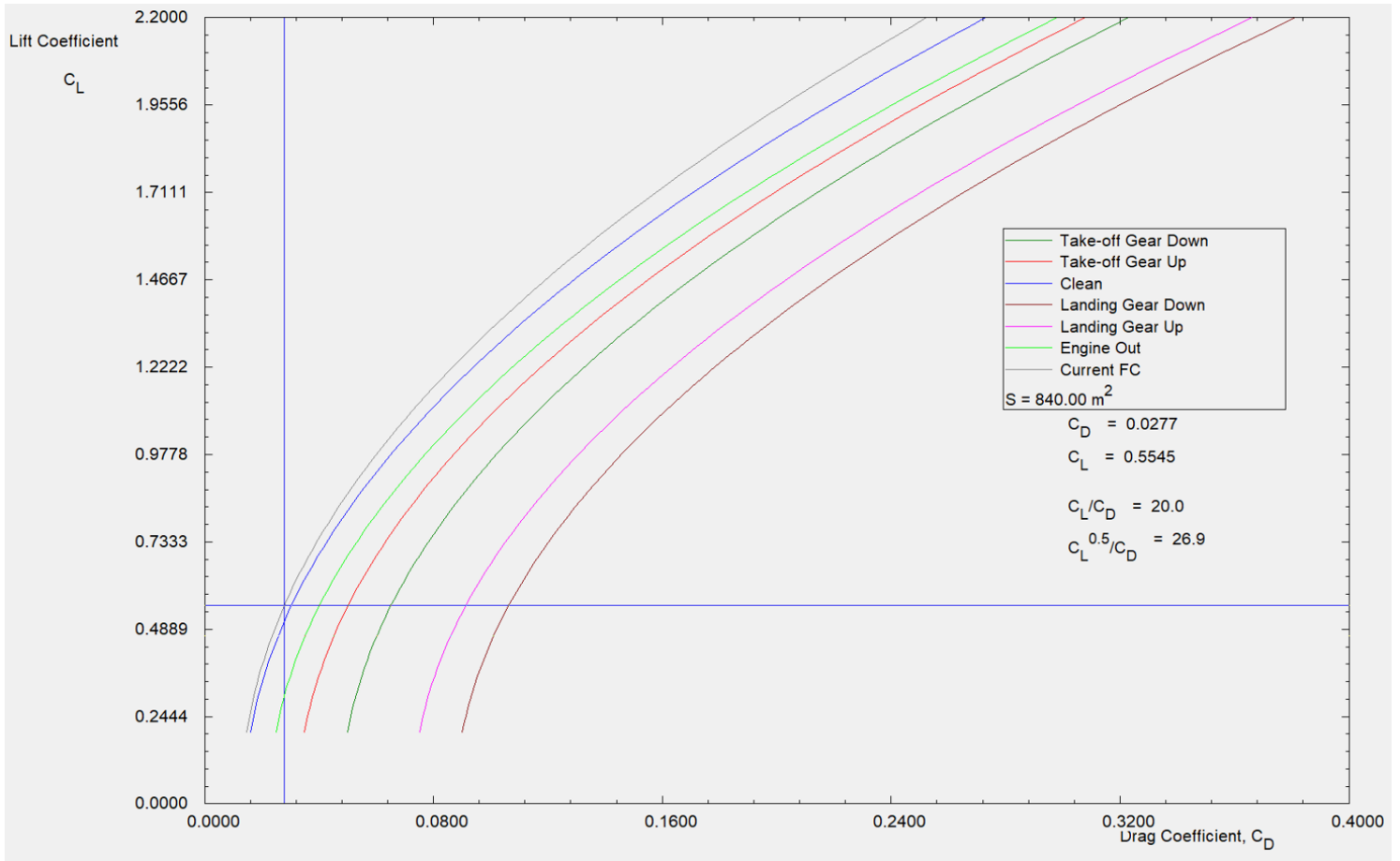


Figure 17. Reassessed Drag Polars. Drag polars reassessed after the bulk of class II analysis and design.

Drag polars have been recalculated based on more detailed class II analysis and the primary consideration of cruise L/D ratio was verified to be within a small margin of the original sizing estimates as this is one of approximately 3 critical performance factors that affect the aircraft's ability to perform its primary mission. The L/D ratio achieved at the primary flight condition matches that determined during the reassessment of the design in section VI.

XII. Propulsion Characteristics

Power from the engines not only propels the aircraft but also feeds a number of other systems, mechanical, electrical and pneumatic and any power used for these systems is unavailable for flight. For an aircraft of this size the usage for non-flight purposes of engine power is small but not insignificant as engines represent a large portion of the aircraft's empty weight. The equations used to calculate this are from Roskam¹ Vol 6 and are shown here.

$$P_{mech_{fp}} = 0.00014 * c_j * \frac{T_{U_{inavail}}}{\eta_{fp}} = 0.00014 * \frac{0.046kg}{N * hr} * \frac{1450000N}{0.65} = 23.62kW \quad (21)$$

$$P_{mech_{hydrau}} = 0.0006 * \Delta P_{hydr} * \frac{V_{hydr}}{\eta_{hp}} = 0.0006 * 2000000 Pa * \frac{350L}{min * 0.75} = 160kW \quad (22)$$

$$P_{elect} = \frac{P_{elec_{requ}}}{\eta_{elec_{gen}}} = \frac{10kW}{0.9} = 11.1 kW \quad (23)$$

$$P_{pneu} = \frac{\frac{\dot{m}_b}{\dot{m}_a} * T_{req} * U_1}{550} = 0.04 * 700000N * \frac{880 \frac{km}{hr}}{550} = 6688.9KW \quad (24)$$

The sum of these extra power expenses is 6.89 MW but could be greatly reduced by utilizing electrical power instead of pneumatic since the bulk of these power expenditures come from the thrust and speed terms in the pneumatic power equation. This is a potential point of improvement for future work on such a design. Even still however, under standard cruise conditions the engines are outputting approximately 123 MW and are producing over 300 MW at peak power output to propel the aircraft so 7 MW is a non-dominating factor while still being large enough to consider.

In class I design the design process the size of the engines was purely a question of how much thrust they can produce and not one of physical expent. With the design calling for engines more powerful than any currently in existence it is necessary to verify that the engines are not excessively large for the aircraft. It is assumed for these calculations that the inlet area is the same as the engine fan frontal area, as is the case for many nacelle mounted engines.

$$A_{inlet} = \frac{\dot{m}_a}{U_1 * \rho} \quad (25)$$

$$\dot{m}_a = 1.06 * K_{BPR} * \left(\frac{T_{TO}}{N_{eng}} \right) \quad (26)$$

To calculate the engine size it is necessary to find the maximum size. To do this the inlet size at takeoff and cruise will be evaluated. K_{BPR} is a factor related to the bypass ratios and is determined empirically, for a BPR of 10 this value is 0.0036¹.

$$A_{inlet_{TO}} = 1.06 * \frac{0.0036s}{m} * \frac{\left(\frac{1400000N}{2} \right)}{\frac{250km}{hr} * 1.2 \frac{kg}{m^3}} = 15.7m^2 \rightarrow D_{inlet} = 4.48m \quad (27)$$

$$A_{inlet_{cr}} = 1.06 * \frac{0.0036s}{m} * \frac{\left(\frac{1400000N}{2} \right)}{\frac{800km}{hr} * 0.38 \frac{kg}{m^3}} = 15.82m^2 \rightarrow D_{inlet} = 4.48m \quad (28)$$

We can see from this that the inlet diameter required for takeoff and for full power at cruise is approximately equal and thus no special precautions need to be taken. This information was calculated at the beginning of class II design and was incorporated into the drag calculations and geometry for the three-views.

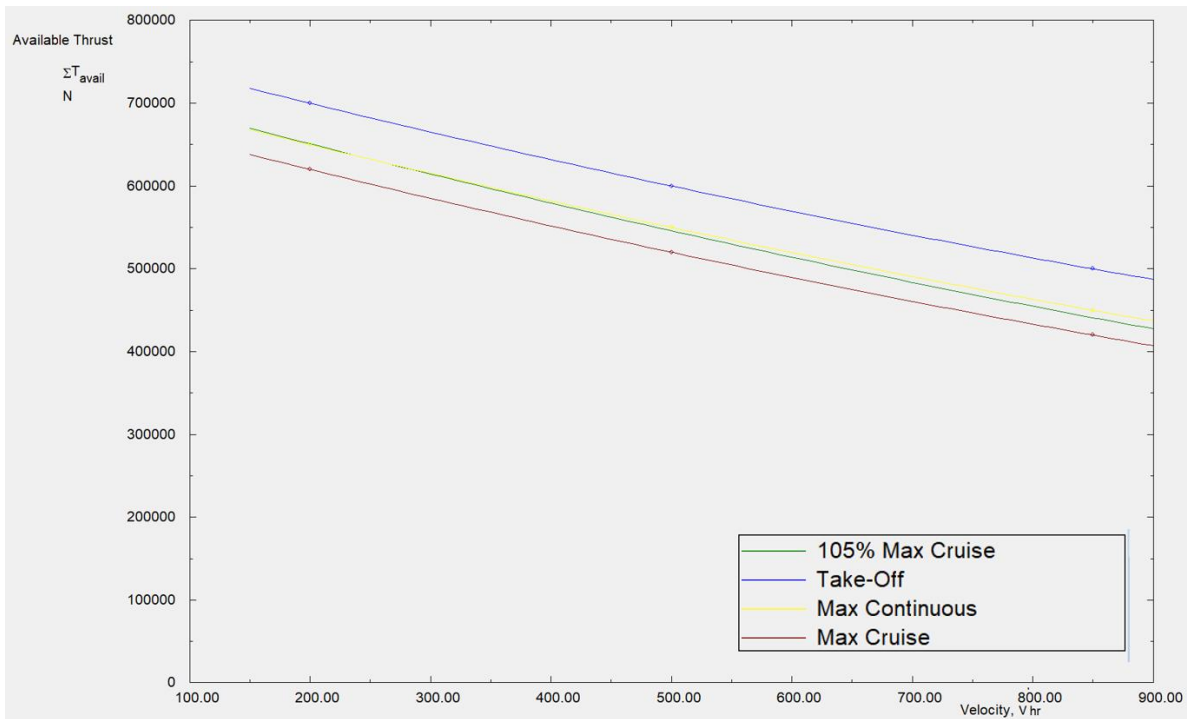


Figure 18. Approximate Thrust-Speed Characteristics at SL. Approximate engine thrust-speed characteristics at sea level

XIII. Performance Evaluation

With the bulk of the design complete it is necessary to assess the ability of the Goliath to meet its designed mission goals. These goals are broken down into sections for discussion their respective values. These calculations were completed within the AAA software suite and utilize the equations presented in Roskam¹ for their completion. The original mission specifications for this aircraft are shown below in table 10 (identical to table 3). Performance for this aircraft is evaluated at 1500 and 0 meters for landing and takeoff operations and 11000 meters for enroute operations (maneuver, cruise speed, etc)

Table 11. Aircraft Specifications. Comparison of C5-M and Goliath Specifications

SPECIFICATION	C5-M ²	GOLIATH
MAXIMUM PAYLOAD (KG)	122472	130000
CRUISE SPEED (KMPH)	833	900
CRUISE ALTITUDE (M)	10600	10700
TAKEOFF ROLL (M)	2600	2600
LANDING ROLL (M)	1100	1400
RANGE*	8056	8000
*C5-M STATED RANGE AT 54431 KG, GOLIATH AT 120000 KG		

A. Takeoff

Takeoff performance makes use of several different equations. These equations are shown below and their results are tabulated at the end of the section with all other performance parameters. These equations are those presented in Roskam¹ and utilized by the AAA¹⁰ software used to compute these calculations.

$$S_{TO} = F_{TO} h_{obs} \left\{ \frac{1}{\gamma_{LOF}} + \frac{\left(\frac{V_3}{V_{S_{TO}}} \right)^2 \left(\frac{W}{S} \right)_{TO} \left\{ \left(\frac{\bar{T}}{W} \right)_{TO} - \mu_g + \frac{0.72 C_{D_o TO down}}{C_{L_{max TO}}} \right\}^{-1} + 1.414}{h_{obs} \rho g C_{L_{max TO}} (1 + 1.414 \gamma_{LOF})} \right\} \quad (29)$$

T

$$S_{TOG} = \frac{\frac{V_{LOF}^2}{2g}}{\left(\frac{\bar{T}}{W} \right)_{TO} - \left(\mu_g + \frac{0.72 C_{D_o TO down}}{C_{L_{max TO}}} \right)} \quad (30)$$

$$\bar{T} = 0.75 T_{set} \frac{5 + BPR}{4 + BPR} \quad (31)$$

$$V_S = \sqrt{\frac{2 \{ W_{current} - T_{set} \sin(\alpha_{current} + \phi_T) \}}{\rho S_w C_{L_{max}}}} \quad (32)$$

$$V_{LOF} = 1.2 V_{S_{TO}} \quad (33)$$

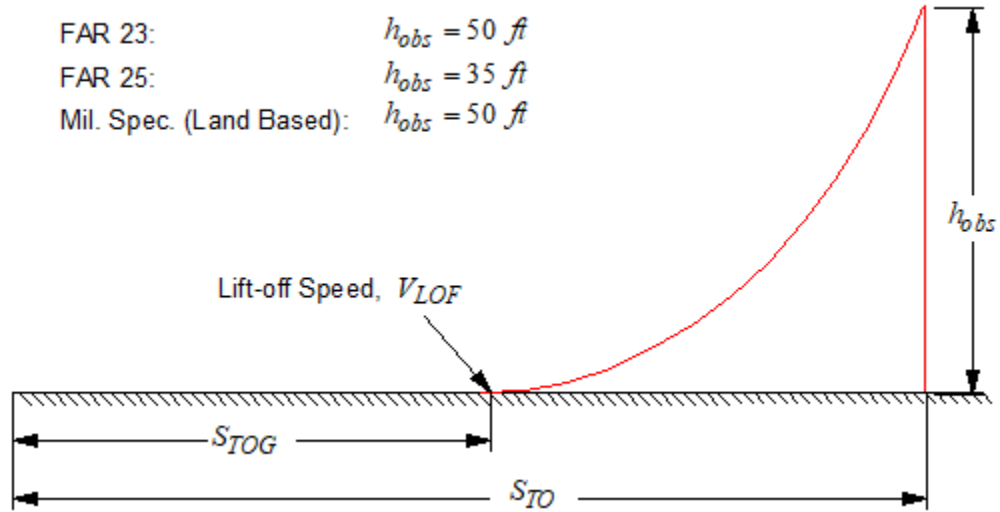


Figure 19. Takeoff Field Geometry. Geometry used for takeoff calculations.

These equations use the normal geometry terms for a takeoff roll and this aircraft uses a 50 ft obstacle for these calculations. This geometry is shown in figure 19 as is presented in Roskam¹ and used in the calculations here.

B. Cruise

The performance in cruise mostly relates to the aircraft's maximum speed in cruise at a specific altitude. The cruise altitude for this aircraft is 11 km. The calculation for determination of maximum cruise speed is straightforward and is shown in the equations below.

$$T_{reqd} = \frac{1}{2} \rho V_{cr}^2 C_{D1} S_w \quad (34)$$

$$T_{avail} = A_{Thrust} V_{cr}^2 + B_{Thrust} V_{cr} + C_{Thrust} \quad (35)$$

$$C_{L1} = \frac{W_{cr}}{q S_w} \quad (36)$$

$$\bar{q} = \frac{1}{2} \rho V_{cr}^2 \quad (37)$$

$$C_{D1} = C_{D0} + B_{CD1} C_{L1} + B_{CD2} C_{L1}^2 + B_{CD3} C_{L1}^3 + B_{CD4} C_{L1}^4 + B_{CD5} C_{L1}^5 \quad (38)$$

The results of solving these equations and graphing the thrust available and thrust required versus flight speed are plotted below in figure 20.

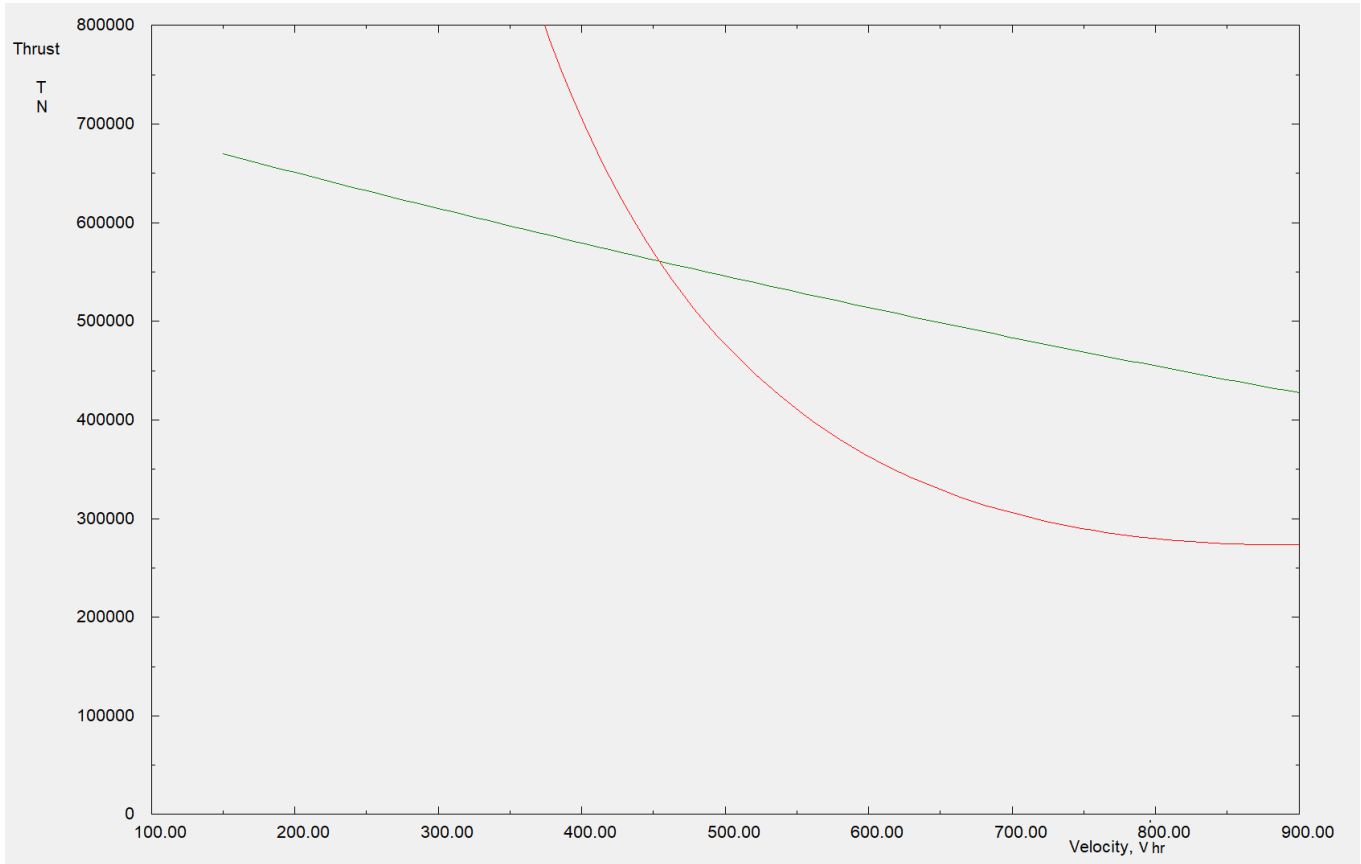


Figure 20. Thrust Available vs Required.Graph of thrust available vs thrust required at cruise altitude.

In addition to cruising speed, at the specified cruise speed range is also a factor. Using the thrust required at speed and the specific fuel consumption of the engine it is possible to approximate the range of the aircraft at steady cruising speed. The results of this calculation are presented in the summary at the end of this section

Endurance is much the same way except the speed and flight attitude used are different from those for maximum range since a different quantity is being maximized.

Varying the range equation for tradeoffs between fuel load and payload produces a graph allowing the determination of maximum range for any given payload. This result is shown below in figure 21.

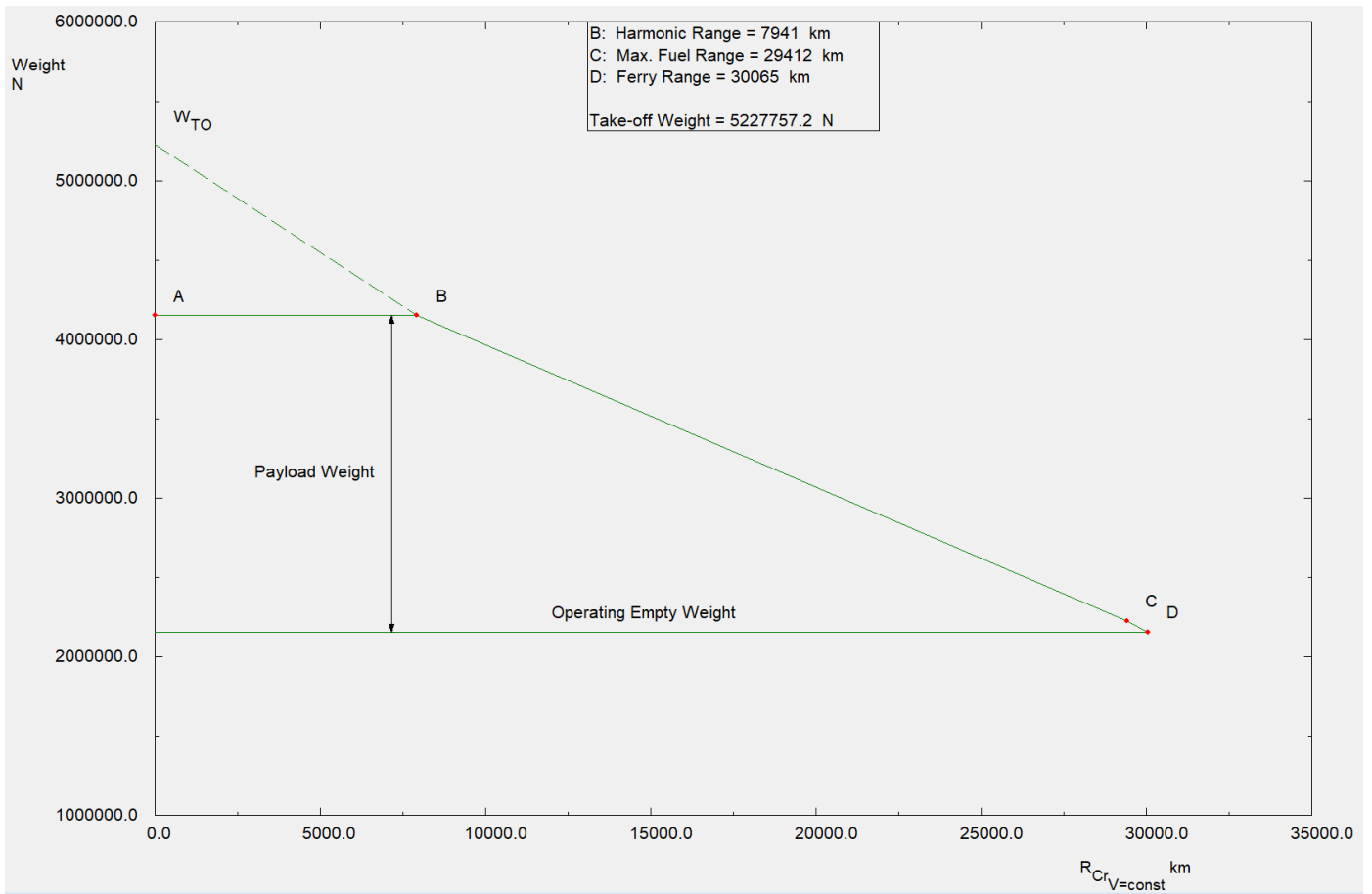


Figure 21. Payload vs. Range. Payload vs fuel tradeoffs and their effect on maximum range.

C. Landing

Landing performance is critical for virtually any aircraft since runways have limited lengths, for the mission of the Goliath it is even more critical since military transports must at times get into facilities and locations without typical infrastructure in place. For this reason landing performance had been a driving concern over and above the takeoff performance for this design. To assess the landing distance of the design. To assess the design the process from Roskam¹ is again used. The equations used in this process are shown below, their implementation fairly obvious.

$$S_{air} = \frac{1}{\bar{\gamma}} \left[\left(\frac{V_A^2 - V_{TD}^2}{2g} \right) + h_{obs} \right] \quad (39)$$

$$\bar{\gamma} = \frac{0.5 \rho V_A^2 S_w C_{DA} - T_{set}}{W_L} \quad (40)$$

$$C_{DA} = C_{D_{oL_down}} + B_{D_{PL_down}} C_{LA}^2 \quad (41)$$

$$C_{LA} = \frac{C_{L_{maxL}}}{f^2} \quad (42)$$

$$V_{TD} = V_A \left[1 - \left(\frac{\bar{\gamma}^2}{\Delta n} \right) \right]^{1/2} \quad (43)$$

$$S_{LG} = \frac{V_{TD}^2}{2\bar{a}} \quad (44)$$

$$S_L = S_{air} + S_{LG} \quad (45)$$

Table 9. Class II Fixed Equip. Component Weights *Breakdown of class II weight estimates for all major fixed system components.*

Parameter	Altitude (m)	Value	Units	Note
Takeoff Field Length	0	2697	m	
Takeoff Field Length	1500	3097	m	
Landing Field Length	0	1004	m	
Landing Field Length	1500	1107	m	
Max Speed	10700	932	km/hr	Mach limited
Max range (const V)	10700	9903.1	km/hr	
Max Endurance (const V)	10700	666.4	min	Maintenance limited with in flight refueling
Stall Speed (TO)	0	243.8	km/hr	
Stall Speed (TO)	1500	262.12	km/hr	
Stall Speed (Landing)	0	193.25	km/hr	

XIV. Cost and Maintenance Evaluation

Table 12. Class II Fixed Equip. Component Weights Breakdown of class II weight estimates for all major fixed system components.

Phase	Cost (Million USD 2050)
Engineering Cost	991.545
Development, Support and Test	430.49
Manufacturing Labor, RDTE	1531.81
Materials, RTDE	226.285
Avionics, RDTE	27
Tooling, RDTE	1584.16
Quality Control, RDTE	199.13
Engine Cost, RDTE	134
Test Operations, RDTE	157.417
Test and Sim Facilities, RDTE	1876.732
Engineering Cost, Manufacturing	583.999
Labor Cost, Manufacturing	6019.965
Materials Cost, Manufacturing	2296
Avionics, Manufacturing	864
Tooling, Manufacturing	866.65
Quality Control, Manufacturing	782.595
Vendor Engines, Manufacturing	4384
Flight Test, Manufacturing	28.8
Fuel, Oil and Lube, Operations	20642.63
Air Crew, Operations	4150
Maintenance Personnel, Operations	4616
Consumables, Operations	666.82
Disposal Cost, Retirement	803.41
TOTAL PROGRAM COST (some items not listed)	80340

The cost estimation for aircraft is based on a huge number of empirical equations derived through statistical analysis of past aircraft costs. Because these equations are neither new nor unique to this design and have a major limitation that precludes them from being held accurate for such a design, these equations will not be presented here. The results of these equations however are presented in table 10. The estimated total production for the program is 80 aircraft produced with 8 produced for research, development, testing and evaluation (RDTE) purposes. The estimated unit cost is 380 Million dollars in 2030 year dollars. The analysis of cost breakdowns is suspect as many of the equations that Roskam¹ puts forth for the cost estimates are empirical based on past information of aircraft; The aircraft used for the trend studies that generated these equations were, at their largest, approximately 80% of the gross takeoff weight of the goliath. These equations have always been intended as approximations but in this instance it is more important than usual to understand this limitation as the approximation for the program cost of the Goliath is significantly looser than it would be for a aircraft designed using the same methods in a more common size band.

XV. Final Geometry

A. Wing

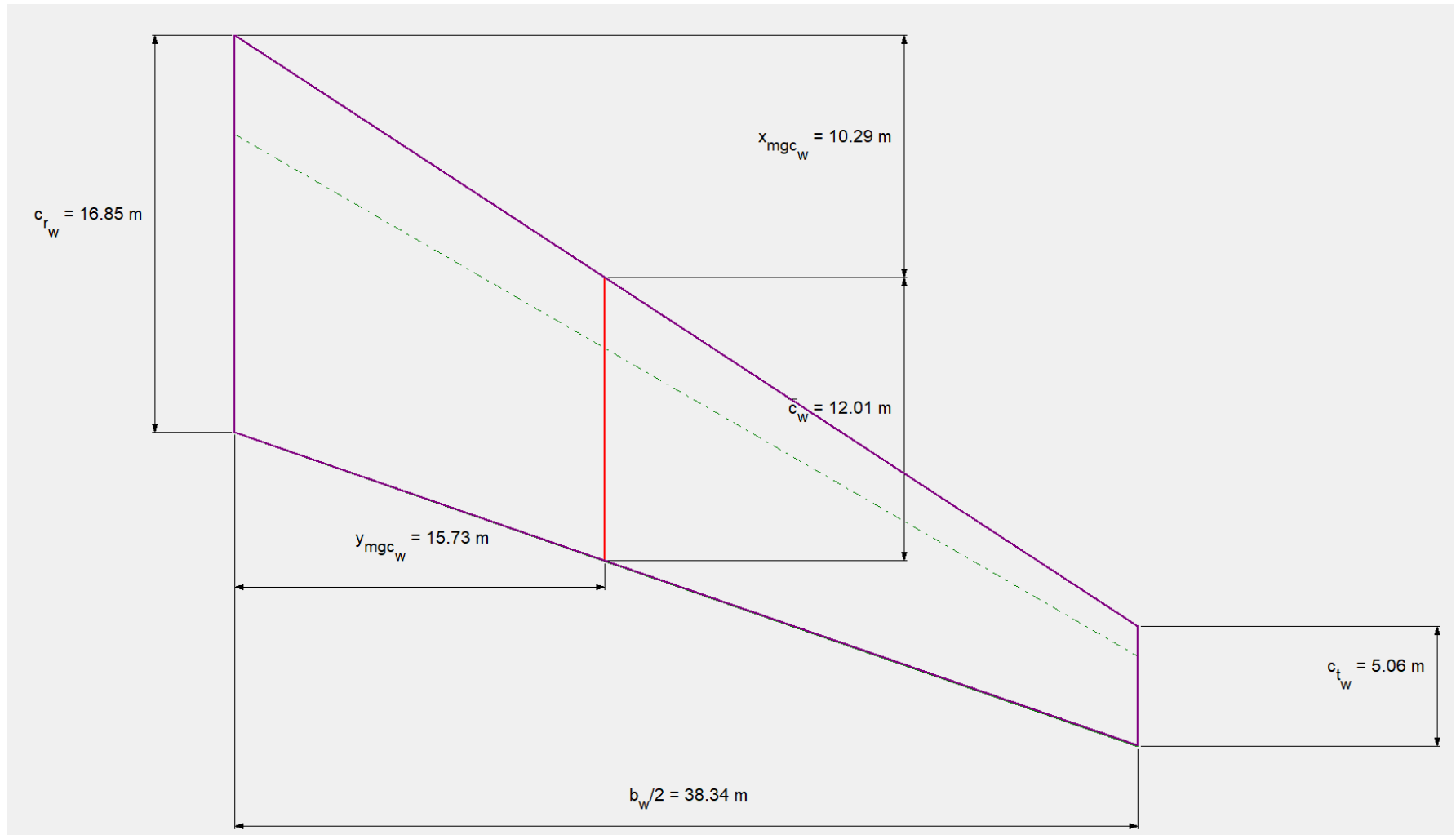


Figure 22. Basic Wing Planform.

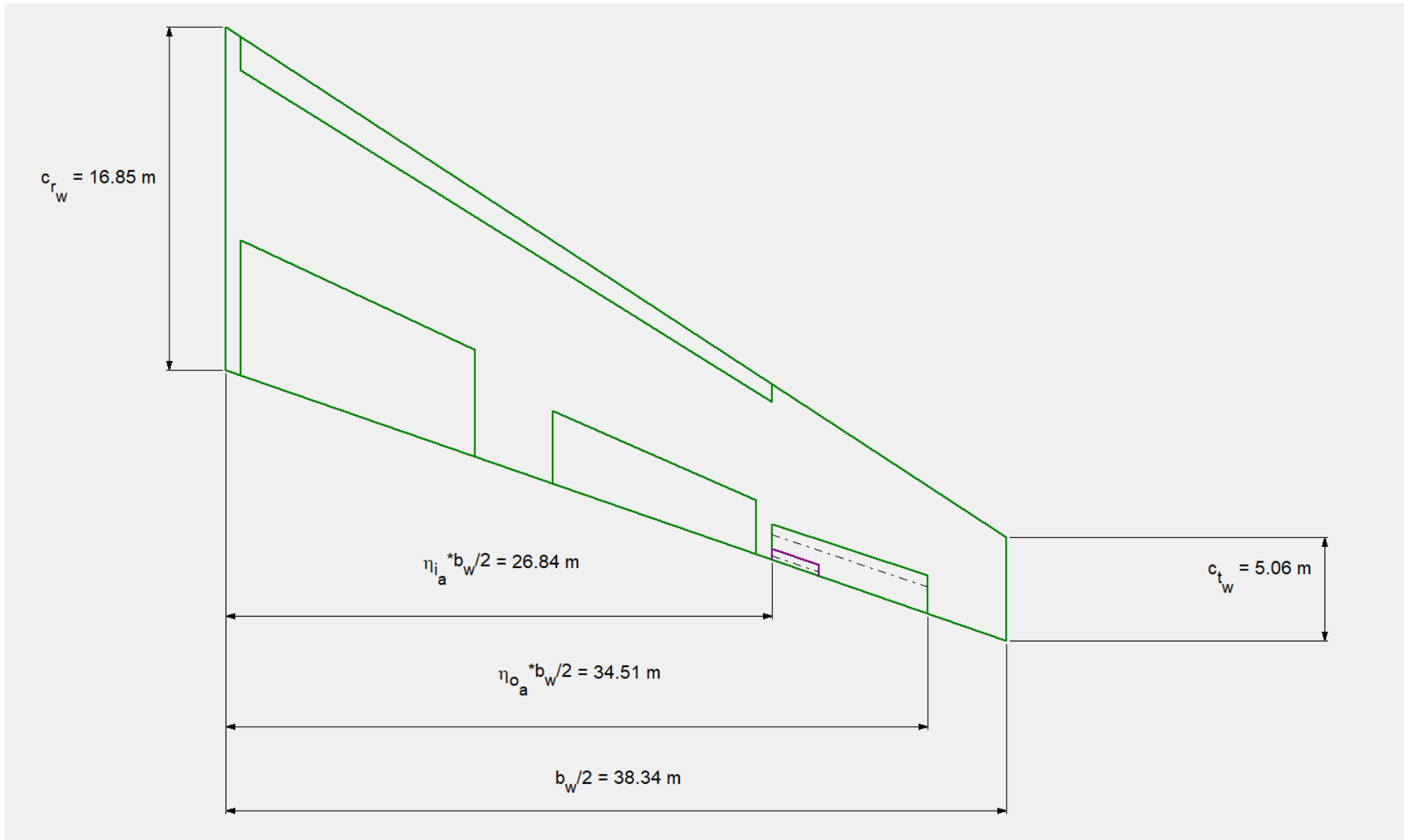


Figure 23. Wing Devices Layout.

B. Horizontal Stabilizer

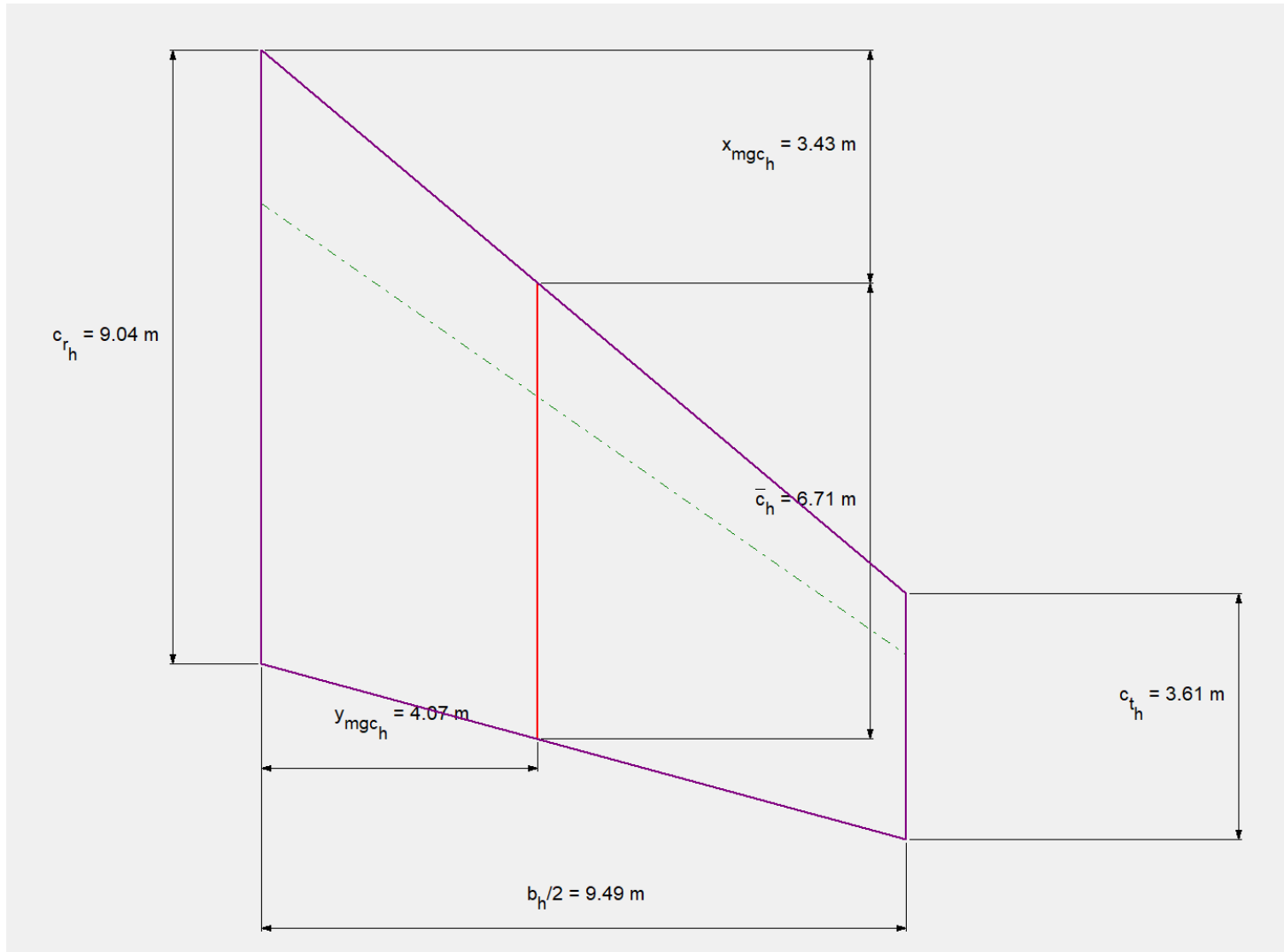


Figure 24. Basic Horizontal Stabilizer Planform Area.

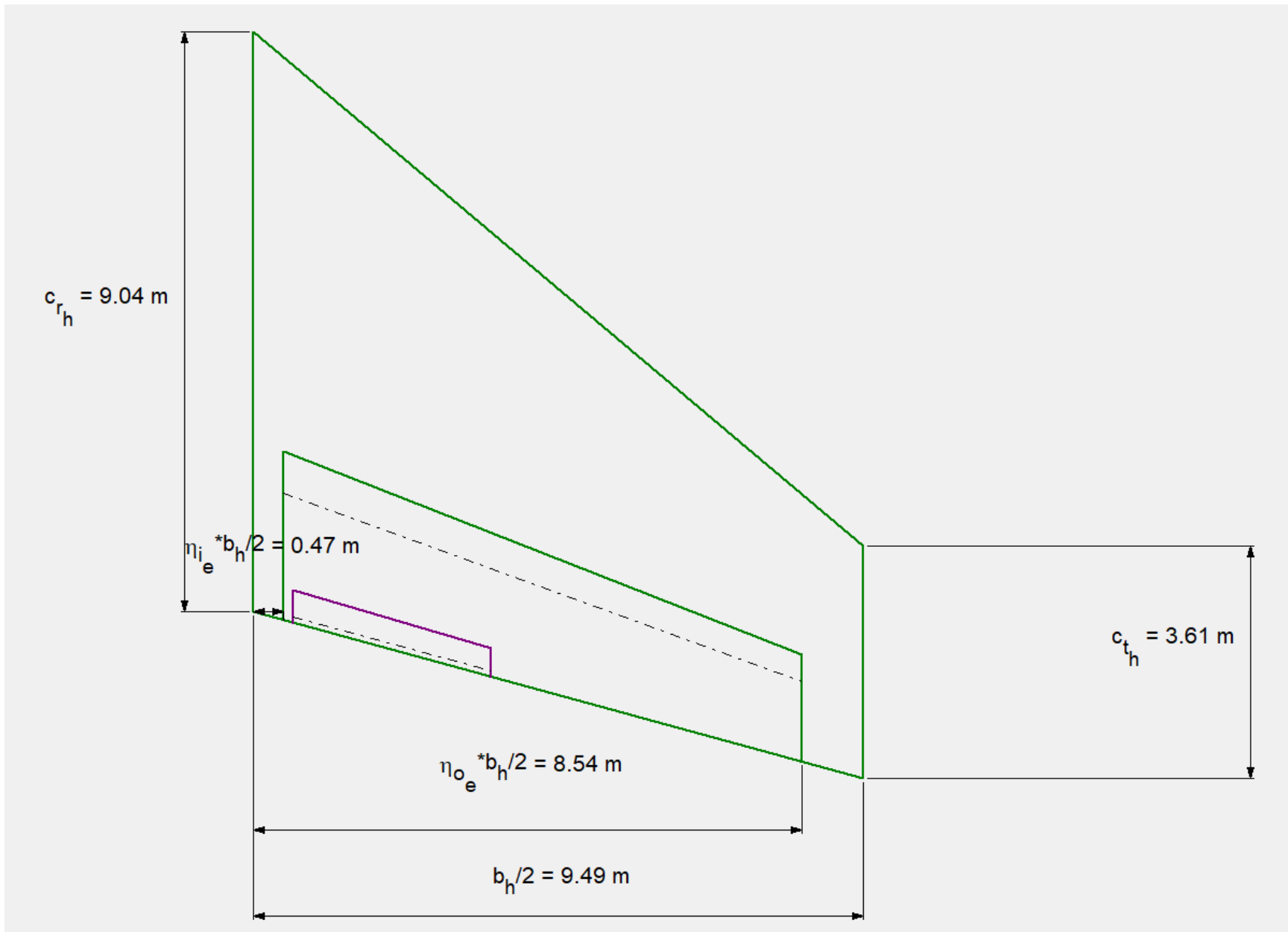


Figure 25. Horizontal Stabilizer Control Surface Layout.

C. Vertical Stabilize

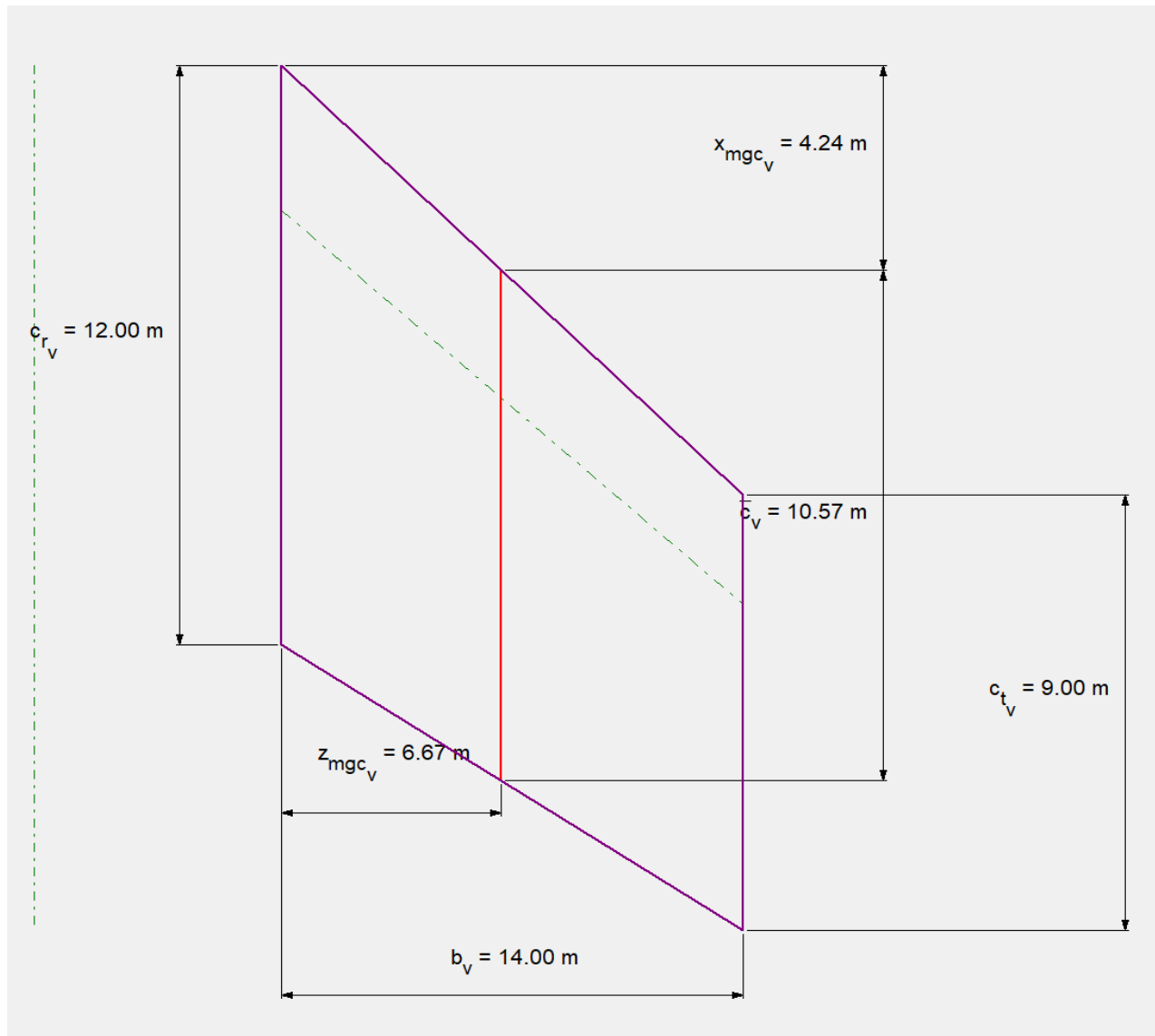


Figure 26. Vertical Stabilizer Basic Layout.

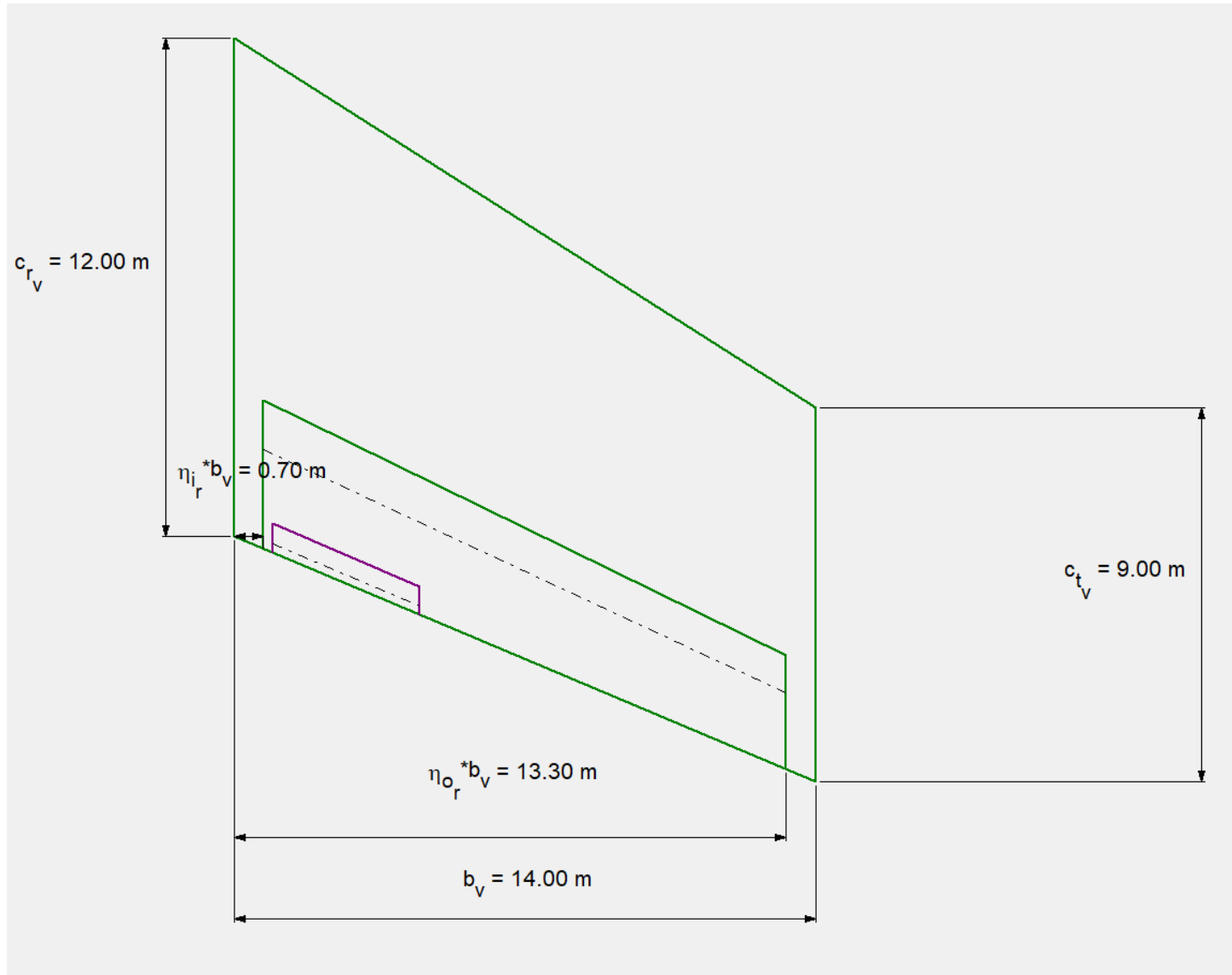


Figure 27. Vertical Stabilizer Control Surface Layout.

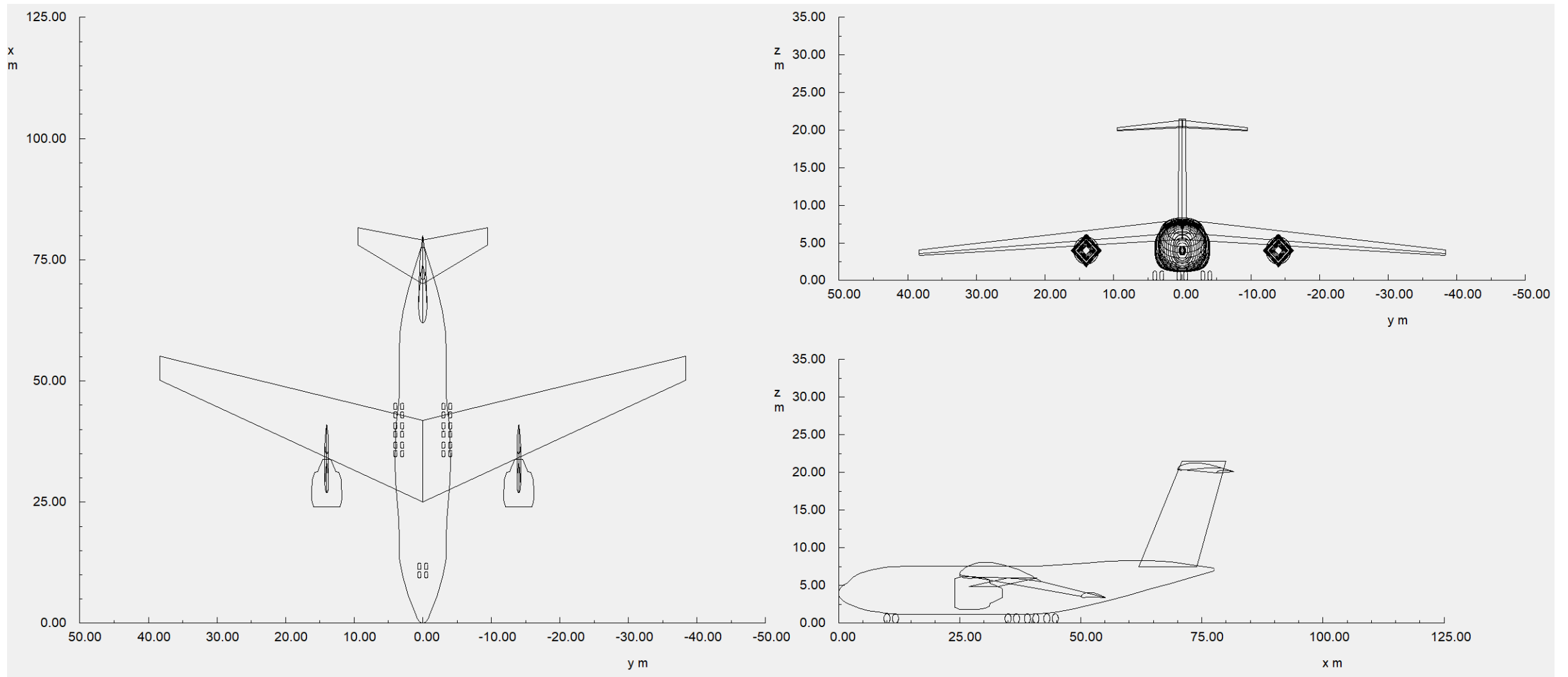


Figure 27. Vertical Stabilizer Control Surface Layout.

XVI. Discussion

While there are some aspects of the design that are less than perfectly refined, the current state of the proposed Goliath design is certain to the point of indicating a feasible design point, it is impossible to state rather it is desirable or not without being the deciding body on such matters (in this case the US Air Force and government) and as such this discussion will proceed under the assumption that it is a desirable design point for their needs.

The design of the Goliath has met its intended design goals and in a couple of cases exceeded them. The landing distance specification was of particular issue during the design and the need for an exceptionally high C_L on landing approach was a driving factor in the wing design, equal with or even ahead of the lift to drag ratio of the wing in importance. The field length restriction on landing has led to an aircraft with an unusually low wing loading for it, similar to the C-5 that inspired the evolution of the design. The wing loading of the Goliath is 6190 pa vs 5940 pa for the C-5 and 7927 pa for the 787-8 that has entered service.

The takeoff requirement produced the single most questionable assumption in the early design that by its very nature propagated to the rest of the design. The assumption that at time of production there would exist a sufficiently powerful engine to power the aircraft with 2 of them. The GE90-115B produced by General Electric is currently the most powerful jet engine in the world and is capable of producing 600 kN of thrust at peak temperature and RPM. The GE90-115B's rating is significantly less than this redline level thrust output at 510 kN. The Goliath requires an engine design capable of producing ~700 kN of installed thrust which requires a 37% increase in engine power. That said however this assumption is not totally unreasonable as jet engines have been continuously increasing in power at a fairly linear rate. This increase in power may be successfully achieved without being demanded by this program. If an engine was not on track to be completed by that time then such a program, likely bankrolled by the US military, would be sufficient to attain development of such an engine. Provisions for this have been made in the design by incorporating weight factors for geared and variable pitch turbofan engines to allow for the use of cutting edge engine technology that negatively impacts weight but allows improved efficiency and power across a wide range of flight conditions.

The speed requirements of the aircraft pushed the design further towards commercial aircraft than previous military cargo transports. Higher sweep angles on the wing require additional structural reinforcement but otherwise have a minimal impact on the design. The difference between the C-5 and the Goliath is relatively small with the wing sweep angle on the C-5 at 25 degrees and the Goliath at 30 degrees. Despite the modest size of the increase it is sufficient to increase the cruise and top speed of the Goliath to 60 kmph greater than the C-5. Wave drag buildup in the transonic region was evident in the later stages of the design analysis and vastly decreases the lift to drag ratio of the aircraft from 20 to 14 with an increase of only about 0.05 Mach above the design cruise speed.

The cost of the program at first glance seems excessive at over 80 billion USD but the development costs of aircraft programs have been steadily increasing due to a complex confluence of factors. For example the F-35 program is projected to cost over 1.5 trillion USD by 2070¹¹. The relatively modest cost of the program (by comparison only) is primarily due to conventional methods intended for the Goliath rather than the highly atypical and cutting edge technologies and methods used to design and construct the F-35 as well as the extremely stringent performance requirements for the F-35 program that required such measures.

XVII. Conclusion

The data presented here is not intended to be a comprehensive detailed list of all details of the design to this point, but rather an overview of the process and results of the design process to this point. Detailed information is contained in the AAA file provided with this document and can also be extracted and presented upon request.

The finalization of the design is quite a ways off if this design were to truly enter detailed design processes however this is a baseline that is suitable for the time and manpower invested to date. Further refinements and investigation into verifying the stability and control properties of the aircraft are necessary as those are the most uncertain quantities of the design but enough analysis on these points had been done to insure they do not grossly affect the layout or sizing and as such small tweaks to improve stability and control can be reasonably assumed to be higher order terms.

A great deal of time in the course of this project was lost due to misinformed decisions on the software to use for physically modeling the aircraft. Original models of the aircraft were done in solidworks and while this was suitable for an overview the lack of detailed mechanical actuation failed to leverage the strengths of Solidworks and the geometry input for AAA⁹ is entirely incompatible with solidworks, requiring the aforementioned great deal of time to translate the geometry into AAA.

Despite not reaching the full extent of the class II design processes, due to misestimations of time required for a number of class II steps, the process completed to date is sufficient to demonstrate the feasibility of this design point well beyond that of a simple class I analysis.

References

- ¹Roskam, J., Airplane design, Lawrence (Kansas): DARcorporation, 2004.
- ²C-5 Specifications. Lockheed Martin. 2017 Retrieved Febuary 2017 from:
<http://www.lockheedmartin.com/us/products/c5.html>
- ³F-35 Specifications and History. Lockheed Martin. 2017. Retrieved Febuary 2017 from:
<https://www.f35.com/about/history>
- ⁴R.P. Hunnicutt, *Abrams: A History of the American Main Battle Tank*. Echo Point Books September 2015.
- ⁵Lange, R.H., Design Concepts for Future Cargo Aircraft, Lockheed-Georgia Company, Marietta, Ga, 1975.
- ⁶Clar T., Dierickx J., Eken K. et al. The HUULC, Design of a Hydrogen-powered Unmanned Ultra Large Cargo Aircraft. Delft University of Technology, Aerospace Engineering. June 2015.
- ⁷Heinze W. and Hepperle M., Future Global Range Transport Aircraft. University of Brunswick. 2003.
- ⁸Airbus A380 Specs. Airbus. 2017. Retrieved Febuary 2017 from:
<http://www.airbus.com/aircraftfamilies/passengeraircraft/a380family/innovation/>
- ⁹Type Certificate Data Sheet E00049EN [GE90-115B]. FAA. June 23 2016.
- ¹⁰Advanced Aircraft Analysis Software V3.7. Darcorp. 2016.
- ¹¹FAA Advisory Circular 150/5300-13, Airport Design